Defining the contribution of microRNA-specific slicing Argonautes in animals

Anisha Pal[1,2], Vaishnav Vasudevan[1,2], François Houle[1,2], Michael Lantin[1,2], Katherine A. Maniates[3], Miguel Quévillon Huberdeau[1,2], Allison L. Abbott[4], Martin J. Simard[1,2,*]

[1]CHU de Québec-Université Laval Research Center (Oncology Division), Quebec City, Quebec, G1R 3S3, Canada

[2]Université Laval Cancer Research Centre, Quebec City, Quebec G1R 3S3, Canada

[3]Waksman Institute of Microbiology and Department of Genetics, Rutgers University, USA;

[4]Department of Biological Sciences, Marquette University, Milwaukee, WI 53233, USA.

*Correspondence: Martin.Simard@crchudequebec.ulaval.ca

Keywords: argonaute, slicer activity, miRNA, *C. elegans*

Alternative title: Characterization of ALG-1 and ALG-2 slicer-argonautes in *C. elegans*

ABSTRACT

microRNAs regulate gene expression through interaction with an Argonaute protein family member. While some members of this protein family retain an enzymatic activity capable of cleaving RNA molecules complementary to Argonaute-bound small RNAs, the role of the slicing activity in the canonical microRNA pathway is still unclear in animals. To address the importance of slicing Argonautes in animals, we created *Caenorhabditis elegans* mutant strains carrying catalytically dead endogenous ALG-1 and ALG-2, the only two slicing Argonautes essential for the miRNA pathway in this animal model. We observe that the loss of ALG-1 and ALG-2 slicing activity affects overall animal fitness and causes phenotypes reminiscent of miRNA defects only when grown and maintained at restrictive temperature. Furthermore, the analysis of global miRNA expression show that the catalytic activity of ALG-1 and ALG-2 differentially regulate the level of specific subsets of miRNAs in young adults. We also demonstrate that altering the slicing activity of those miRNA-specific Argonautes does not result in any defect in the production of canonical miRNAs. Together, these data support that the slicing activity of miRNA-specific Argonautes functions to maintain levels of a set of miRNAs for optimal viability and fitness in animals particularly exposed to specific growing conditions.

INTRODUCTION

The microRNAs (miRNA) are ~21 nucleotides (nt) long non-coding RNAs involved in various biological processes in animals, plants, and fungi, including proliferation and differentiation, development, circadian rhythm, and stress response (1). Typically, miRNAs engage in post-transcriptional gene silencing through a degree of complementarity with sequences typically found in the 3' untranslated region (UTR) of mRNA (2, 3). The production of miRNA involves sequential molecular steps that occur in the cell's nucleus and cytoplasm. First, the primary miRNAs (Pri-miRNA) are transcribed by RNA polymerase II and then are bound and cleaved by the microprocessor complex (Drosha-DGCR8) in the nucleus to generate the precursor miRNA (pre-miRNA) (4) . Once exported into the cytoplasm, Dicer cleaves the pre-miRNA to produce small duplex RNA molecules consisting of the miRNA guide (mature) strand that is then bound by an Argonaute protein and the passenger strand (star miRNA) that is discarded during the loading process onto Argonaute (5–7). After the mature miRNA loading, the Argonaute protein associate with other factors such as TNRC6/GW182 protein to form the miRNA-induced silencing complex (miRISC). The miRISC binds to the complementary 3'UTR of the target mRNA and brings upon various factors to trigger post-transcriptional gene silencing (8). In animals, the miRNA pathway is involved in translational repression and in the degradation of the target through the recruitment of the deadenylase CCR4/NOT complex by TNRC6/GW182 (9). Recently, it has been shown that miRNAs can modulate gene expression in a TNRC6/GW182 independent manner in particular conditions, such as animal embryogenesis (10). Interestingly, along with blocking translation, miRISC binding can also stabilize the targeted mRNAs in the germline by sequestering them at a specific subcellular location through miRISC interaction with GLH-1/Vasa (11). Therefore, it is clear that besides the miRNA molecule and Argonaute, interactors in *cis* and *trans* of the miRISC can modulate its gene regulatory mode of action (12).

The Argonaute protein family represents the functional key player of all small non-coding RNA-mediated gene silencing pathways found across archaea to eukarya. Phylogenetically, there are three major classes of Argonautes: the Argonautes, the PIWI proteins and a set of worm specific Argonautes involved in different small RNA-specific

gene regulatory processes (13). The miRNA-mediated gene silencing implicated members of the Argonaute clade, including Ago1 to 4 in mammals and ALG-1, ALG-2 and ALG-5 in the nematode *Caenorhabditis elegans* (14, 15). The Argonaute proteins contain four major domains: The N-terminus, PAZ (Piwi/Argonaute/Zwille), Mid and PIWI (P-element induced wimpy testis) (16, 17). While the PAZ and Mid domains are required to bind the 3' and 5' end of small RNAs, respectively, the C-terminus PIWI domain can act as an endonuclease which cleaves the phosphodiester bond of the RNA backbone . This enzymatic or slicing activity requires four specific (DEDH) residues (known as catalytic tetrad) within the PIWI domain to bind divalent cation (i.e. Mg+2, Mn+2) and cleave target mRNA if there is near perfect or perfect complementarity with the bound small RNA molecule (14).

Argonaute slicing activity is essential for siRNA-guided target cleavage and for piRNA-mediated genome integrity maintenance in the animal germline (18–24). In contrast to plants, the absence of the perfect complementarity in animals between miRNAs and mRNA targets prevents their cleavage. Interestingly, many Argonautes that bind miRNAs in animals have retained the residues essential for target cleavage (25). Previous reports have suggested some contributions for the slicing activity of Argonautes in the miRNA pathway. For instance, slicing human Ago2 has been demonstrated to be engaged in processing functional miRNAs in cells. In vertebrates, Ago2 cleavage activity has been proven to be involved in producing two specific miRNAs, miR-451 and miR-486, that are essential for erythroid development (26–29). In the case of miR-451, its maturation creates a short hairpin structure, which bypasses Dicer and directly binds Ago2 to be processed into mature miRNA (27–29). On the other hand, miR-486 necessitates Dicer for its maturation but requires slicing Ago2 to eliminate the star strand from the miRNA duplex (26). While those studies highlight the contribution of slicing Argonaute in producing specific miRNAs, some limitations in those approaches prevent understanding the broader impact of the slicing activity of Argonautes in the miRNA pathways in animals. First, Ago2 slicing activity is essential for another small RNA gene silencing pathway that uses siRNA to cleave mRNA targets (30, 31). Next, it has been recently reported that Ago3, another member of the Argonaute family implicated in the miRNA pathway, also

possesses slicing activity (32). Therefore, decoupling the Argonaute slicing activity for siRNA and miRNA production as well as understanding its contribution for miRNA function has remained a challenge in mammalian systems.

Here, we take advantage of the nematode *C. elegans* as an animal model to elucidate the contribution of slicing activity of Argonautes in the animal miRNA pathway. *C. elegans* has three Argonautes phylogenetically related to all four human Argonautes that are exclusively implicated in the miRNA pathway, ALG-1, ALG-2 and ALG-5 (33–35). However, out of these three, only ALG-1 and ALG-2 carry the four residues essential for slicing activity (Figure 1A) and are catalytically active (36). Therefore, we created animals deprived of ALG-1 and ALG-2 slicing activity and studied their contributions to the miRNA pathway. We found that their catalytic activity had important effects on animal fitness and different developmental pathways controlled by miRNAs when maintained in stressful conditions. We also observed that ALG-1 and ALG-2 slicing activity regulate the abundance of specific miRNAs and thus without causing any defect in their production.

MATERIAL AND METHODS

Worm Culture and phenotypic studies

All *C. elegans* strains were cultured and handled using standard protocol (37). All strains were grown on solid nematode growth media (NGM) Petri and fed with *E. coli* OP50. Worms were maintained at 15°C unless specified. Hermaphrodite animals were used for the experimental purpose unless indicated otherwise. The specific life stage for each experiment is mentioned in the respective figure legend. Brood size, alae defect, gonadal arm migration and lifespan assays were done at 25°C after keeping the worms at 25°C for at least 3 generations. *alg-1(null)* and *alg-1(null); alg-2(CD)* animals were grown at 20°C for 2-3 generations and transferred at the L1 stage at 25°C for one generation to do phenotypic analysis.

Mutant generation by CRISPR-Cas9 system

Genome editing of *C. elegans* by CRISPR-Cas9 method was done as previously described (38). F1 heterozygote and F2 homozygotes mutants were identified by using PCR genotyping and Sanger sequencing. All newly generated strains by CRISPR-Cas9 were outcrossed twice at least. All the strains, used for this study and details of primers and oligonucleotide sequence for genome editing are listed in Table S1-S5.

Lifespan assay

All strains were synchronized by alkaline hypochlorite solution treatment. For the lifespan assays, 25 to 30 L1 animals were plated on NGM plates containing OP50 and let for growth at 25°C. At the L4 stage, animals were transferred to NGM plates (with OP50) with FUDR (50μM). Adult worms were transferred every 2 days during active reproduction and scored for viability. Animals were scored as dead when they stopped responding to gentle prodding with a platinum wire pick. Dead animals were removed from the plates. Animals that died by internal hatching, vulval bursting, or crawling on the side of the plates were censored from the lifespan analysis. *p*-values were calculated using the Gehan-Breslow-Wilcoxon method.

Sperm quantification

GFP tagged histone was used to visualize the spermatids. Argonaute CD mutants were crossed with strain (RF1025), carrying a GFP tagged histone transgene, *stls10027*, to quantify the spermatids. L4 hermaphrodites were upshifted from 20°C to 25°C and their progeny was analysed for the number of sperm that they generated. Sperm quantification was completed following the outline, mentioned in Huang et al, 2012 and Maniates et al, 2021 (39, 40), where L4m+4-hour animals were smashed on a slide in sperm medium and then GFP positive spermatids were counted.

Embryo and Young adult collection

Synchronised worm population was collected using alkaline hypochlorite treatment and later collected in M9 solution. We collected embryos (for immunoprecipitation) and young adults at 25°C, after keeping the worms at 25°C for at least 3 generations. For RNA extraction the worm pellets were snap-frozen in Trizol. For Protein extraction the worm pellets were snap-frozen in M9.

Protein Extraction

Extracts were prepared from synchronized young adult animals as well as embryos. Worms suspended and frozend in M9 solution were washed and resuspended in cold lysis buffer (10mM Potassium Acetate, 25mM Hepes-Potassium Hydroxide pH 7.0, 2mM Magnesium Acetate, 1mM DTT, 0.5% [v/v] Triton X-100 and protease inhibitors) before being lysed by shaking with (Next Advance RINO) bead lysis kit using bullet blender Storm 24. Then the extracts were centrifuged at 17,000g for 20min at 4˚C and the clarified supernatants were collected and processed for Western Blot or Immunoprecipitation.

Immunoprecipitation

Protein quantification was done using Bio-Rad Protein Assay. For immunoprecipitation, Dynabeads protein-G (Thermo Fisher Scientific) was washed three times using cold lysis buffer and then incubated with ALG-1 antibody in 250µl lysis buffer for 1 hr at room temperature with rotation. Antibody tagged Dynabeads were washed thrice with lysis buffer and then incubated with protein extract for overnight at 4ºC with rotation. For endogenous flag tagged ALG-2 immunoprecipitation, we used anti-FLAG M2 magnetic beads (Millipore Sigma) directly.

Western Blotting

Equal amounts of proteins or beads were resuspended in 2X SDS loading buffer (100mM Tris-HCl [pH 6.8], 4% [w/v] SDS, 200mM DTT and 20% [v/v] glycerol) and then heated at 95˚C for 10 min. Samples were resolved onto an 8% SDS-PAGE and transferred to Protran Premium NC membranes (GE Healthcare). The membranes were blocked with

milk (5% [w/v] dried milk in 1X PBST and were incubated overnight at 4˚C with primary antibodies. Rabbit polyclonal anti-ALG-1 and anti-AIN-1 antibodies were used at 1:1000 and 1:2000 dilution respectively in 1% (w/v) dried milk supplemented PBST. Monoclonal mouse anti-beta-ACTIN (Abcam, ab49900) antibody was used at 1:20000 dilution in 1% (w/v) dried milk supplemented PBST. Anti-FLAG (Millipore Sigma, F1804) antibody was used at 1:10000 dilution in 1% (w/v) bovine serum albumin supplemented PBST. Membranes were then incubated with appropriate secondary antibodies before developing with Perkin-Elmer ECL Western Lightning Plus solution and visualized using Chemidoc imaging system (BioRad).

Assessment of Argonaute expression and proteasomal degradation

Synchronised young adult worms were treated by rotating them in suspension for two hours with vehicle only (DMSO) or with 100μM MG132 (Sigma-Aldrich, 474790) in M9 buffer. Then, the worms were collected and washed in M9 before being lysed in SDS loading buffer.

RNA isolation and Northern Blot

Trizol (Millipore Sigma) was used to extract total RNA from frozen worm pellet or from beads after immunoprecipitation. Before Trizol extraction, those beads were suspended in 2X PK buffer (100 mM Tris-Cl [pH 7.5], 200 mM NaCl, 1% [w/v] SDS) and digested with proteinase K at 50°C for 20 minutes. 10-12 micrograms of total RNAs were used for northern blot. Samples were mixed with an equal volume of 2x Loading Dye (8M urea, 25 mM EDTA, 0.025% [w/v] xylene cyanol, 0.025% [w/v] bromophenol blue) and heated 5 minutes at 80°C. 15% Urea Gel PAGE (Sequagel solutions) was pre-ran for 25 minutes before loading the samples. The gel was transferred onto GeneScreen Plus Hybridization Transfer Membrane (Perkin Elmer). The RNA was cross-linked to the membrane with an EDC solution [0.373g (1-ethyl-3-(3-dimethylaminoprophy) carbodiimide and 1x methylimidazole (127.5 mM 1-methylimidazole-HCl [pH 8]) at 60°C for 1 hour. The membrane was then washed with water several times and baked at 80°C for 10 minutes.

The membrane was pre-hybridized in a hybridization bottle with 25 mL (5X SSC, 20 mM Na_2HPO_4 [pH 7.2], 7% [w/v] SDS, 2X Denhardt's Solution and 1 mg of freshly denatured sheared salmon sperm DNA) at 50°C for 2.5 hours with rotation. Probes (found in Table S6), radiolabelled using Reaction Buffer (10mM Tris-HCl, 5mM $MgCl_2$, 7.5mM DTT pH 7.5) and Exo-Klenow DNA polymerase (NEB); and Stop Solution (10mM EDTA) (IDT StarFire protocol) were heated at 85°C for 5 minutes, directly added to the membrane and incubated in fresh pre-hybridization solution overnight at 50°C with rotation. The membrane was washed three times in stringent wash solution (3X SSC, 5% [w/v] SDS) and once with non-stringent wash solution (1X SSC, 1% [w/v] SDS), at 50°C with rotation. Phosphorimager screen was exposed to the membrane and revealed by autoradiography. Membranes were stripped by adding 100 mL of boiled 0.5% [w/v] SDS solution and incubating at room temperature for 10 minutes twice and they were re-used again for hybridization after confirming the removal of the probe by exposure.

miRNA cloning, sequencing, and analysis

We used NEBNext multiplex small RNA library kit for small RNA library preparation from young adults total RNA extracts and from IP samples (samples are listed in Table S7-S8).

The small RNA sequencing data are available on Gene Expression Omnibus (GEO) with the accession number: GSE222733. Hiseq 4000 SR50 sequencing reads were mapped to the genome and cDNA using custom PERL (5.10.1) scripts and Bowtie 0.12.7 (41). Databases used include *C. elegans* genome (WormBase release WS215), Repbase 15.10 (42), and miRBase 16 (43). The Generic Genome Browser (44) was used to visualize the alignments. The samples were normalized to the total small RNAs including miRNAs, 22G-RNAs and 21U-RNAs (normalized reads can be found in Table S9-S10). All miRNA sequencing analysis was performed using R Statistical Software (v4.2.1; R Core Team 2022). Differential expression analysis was performed using Rankprod package (v3.22.0) and miRNAs with p Values ≤ 0.05 were considered significant. The log2 Normalised Reads Per Million are Z score transformed for generating Heatmaps with

ComplexHeatmap package (v2.12.1). Spearmans rank correlation was visualized using Corrplot package (v0.92).

RESULTS

Catalytically inactive miRNA-specific Argonautes impact animals' fitness

To elucidate the role of the endonuclease slicing activity of miRNA specific Argonautes in animals, we replaced the first aspartate of catalytic tetrad with alanine in endogenous *alg-1* and *alg-2* using CRISPR-Cas9 gene editing, as the other miRNA-specific Argonaute, ALG-5, does not carry essential residues needed for endonucleolytic cleavage (Figure 1A). This point mutation is known to abrogate the slicing activity in Argonautes (26, 27, 29, 31, 45) and does not affect the steady-state levels of ALG-1 and ALG-2 (Figure S1). Besides animals expressing either ALG-1 or ALG-2 catalytic dead (CD) Argonautes, we also generated different double mutant animals to take into consideration the partial redundancy seen for *alg-1* and *alg-2* (33, 45–48) (Figure 1B).

When we monitored animals within the population for each genotype that display health issue (such as developmental arrest and protruding vulva), we observed that only animals expressing ALG-2(CD) without *alg-1* show any reduced fitness to a level greater than seen in *alg-1(null)* animals at standard growing conditions (20°C; Figure 1C). As increasing growing temperature creates physiological stress (49, 50), we next surveyed the phenotypes of the different mutant animals maintained for at least three generations at 25°C. In this specific condition, while single *alg-1* and *alg-2* catalytically dead animals displayed no significant defects, all animals expressing both ALG-1 and ALG-2 slicing dead Argonautes were sick, with a portion of these mutants dying before reaching adulthood mainly due to larval death and bursting (Figure 1D). We also detected that expressing ALG-1(CD) in the absence of *alg-2* causes significant defects in a portion of the population, notably prominent egg laying defects (Figure 1D; as *alg-1(null)* cannot survive at 25°C, we were unable to score any mutant animals at this temperature). We thereafter pursued the phenotypic and molecular characterizations of ALG-1 and ALG-2

catalytically dead mutant animals from populations maintained at 25°C, unless specified otherwise.

Next, we monitored the brood size of those different animals and observed that the brood size of animals expressing either one or two miRNA-specific mutated Argonautes significantly decrease when compared to wild-type (Figure 1E). The quantification of sperm and unfertilized oocytes of animals with significantly low brood size indicates that the decrease in brood size is not caused by either a decline of sperm number or fertilization defects (Figure S2) but likely rather by defect(s) during oogenesis or embryogenesis. We conclude that the loss of the catalytic activity of both miRNA-specific ALG-1 and ALG-2 alters fitness and fecundity in *C. elegans* when maintained at more stressful growing conditions.

The slicing activity of ALG-1 and ALG-2 contributes to miRNA function in animals

To next determine whether the slicer activity of ALG-1 and ALG-2 contribute to known miRNA-mediated gene regulatory pathway in animals, we first monitored the effect of the ALG-1 and ALG-2 CD mutation on alae structure of young animals. This cuticle structure is generated by seam cells at the L4 to adult transition. The proper timing and differentiation of seam cells in larval development requires specific miRNAs, including *lin-4* and *let-7* miRNA family (33, 47, 51–54). The alteration of miRNA function in the process leads to an abnormal number and defective fusion of seam cells, causing incomplete alae breaks along the structure (55–57). When compared to wild-type animals, single as well as double mutants of catalytic dead Argonautes showed a significant increase in alae defects, and the effect of ALG-1(CD) is exacerbated by the loss of *alg-2* (Figure 2A). This data suggest that the alteration of this enzymatic activity affects the function of miRNAs in this developmental process.

Another anatomical structure that requires miRNA activity is the *C. elegans* hermaphrodite gonads. In this case, two miRNAs, miR-34 and miR-83, contribute to the appropriate migration of distal tip cells (DTC) of gonadal arms (58, 59) to create the distinctive U-Shape structure found in adult animals. We observed that while the loss ALG-1 catalytic activity alone does not influence the proper migration of animal gonads,

the catalytic activity of ALG-2 is needed for this process (Figure 2B). Since the loss of both ALG-1 and ALG-2 slicing activity does not cause an additive effect, we conclude that ALG-2 slicing activity is the most important contributor to this process.

Next, it has been reported previously that ALG-1 (53, 60, 61) and specific miRNAs (62–68) are implicated in *C. elegans* lifespan regulation. We, therefore, wanted to determine whether the catalytic activity of ALG-1 and ALG-2 is involved in animal aging. As reported before (60), we observed that only the loss of *alg-1* but not *alg-2* leads to a shortened lifespan (Figure 3A-B). When we surveyed the single or double *alg-1* and *alg-2* catalytically dead mutants, we did not observe any significant effect on lifespan (Figure 3C-G). Altogether, our data suggest that the slicing activity of ALG-1 and ALG-2 contributes to specific miRNA functions in animals.

Catalytic dead ALG-1 and ALG-2 affect levels of specific miRNAs in young adults

Previous studies in mice have shown that two erythroid-specific and atypical miRNAs necessitate the slicing activity of Ago2 to be correctly processed (26, 27, 29). To determine the broader contribution of miRNA-specific Argonaute in animals, we measured the abundance of miRNAs in young adults carrying ALG-1 and ALG-2 catalytically dead Argonautes by high-throughput sequencing.

A total of 176 detected miRNAs were detected and after the removal of miRNAs showing near zero variance across all samples, 162 miRNAs were taken for further analysis. By comparing the total miRNA profile of each genotype, we found that *alg-1(CD)* and *alg-1(CD); alg-2(CD)* animals have similar expression profiles when compared to either *alg-2(CD)* or wild-type animals (Figure 4). Among the genotypes, the *alg-1(CD)* and *alg-1(CD); alg-2(CD)* animals were also the only samples showing a significant positive spearman correlation with each other (Figure S3A). This trend in expression was observed even when the analysis was performed only on the significant dysregulated miRNAs obtained when the individual genotypes were compared with the same wild-type animal baseline expression profile (Figure 5A). We also observe an increased correlation

coefficient among all the genotypes when using only the significant dysregulated miRNAs (Figure S3B). This indicates that while the loss of either ALG-1 or ALG-2 catalytic activity leads to striking differences in the expressed miRNA pool in animals, the loss of both ALG-1 and ALG-2 activity, show more similarities in affected miRNAs with *alg-1(CD)* than *alg-2(CD)* animals.

Among the 47 significantly dysregulated miRNAs when compared to wild-type, we identified 13 up-regulated and 11 down-regulated miRNAs (Figure 5B-C). In contrast, the expression levels of star strand miRNAs, did not show such a striking trend in dysregulation which can be due to their low abundance causing variability within replicates for each genotype (Figure S4). We therefore conclude that altering the slicing activity of ALG-1 and ALG-2 causes alteration in the level of specific subsets of miRNAs in young adult animals.

Next, to determine if miRNA production is affected in the absence of catalytic miRNA-specific Argonautes, we monitored the level of precursor and mature miRNA molecules by Northern blots. When we probed for specific miRNAs in animals expressing ALG-1 and ALG-2 CD Argonautes, we did not observe any accumulation of pre-miRNA precursors in any condition (Figure S5). Thus, even though altering both ALG-1 and ALG-2 slicing activity affects the level of a subset of miRNAs, it does not cause either accumulation of miRNA precursor molecules (as observed in their complete absence (57, 68) or create truncated miRNA precursors as seen when overexpressing catalytically inactive ALG-1 or ALG-2 (57). Altogether, these results suggest that the loss of ALG-1 and ALG-2 slicing activity has a different effect on miRNA levels in animals which is not caused by a defect in miRNA production.

DISCUSSION

In this study, we explored the actual global contribution of slicer Argonautes in the miRNA pathway. Previous studies in mammals only showed that the slicer Argonaute Ago2

participated in the biogenesis of two distinct and atypical miRNAs, miR-451 and miR-486 (26–29). Importantly, those studies could not exclude the contribution of the Ago3, another Argonaute binding miRNAs with slicing capacity (32). Furthermore, Ago2 is also needed in the mammalian system for other small RNA pathways, such as siRNAs (30, 31), which complicated the phenotypical analyses of the Ago2CD mutant. Thus, the studies so far have prevented the precise analysis of the contribution of slicing Argonautes to the miRNA pathway in animals. The use of *C. elegans* represents the ideal system for elucidating the slicing Argonautes function in the miRNA pathway, as ALG-1 and ALG-2 are essential for this regulatory pathway and are not involved in other small RNA pathways in this animal model (33, 34).

A previous study has reported that the slicing activity of ALG-1 and ALG-2 was essential for animal viability (36). In contrast, our data here supported that the slicing activity of ALG-1 and ALG-2 has a more modest contribution in animals grown in optimized conditions. The discrepancy between those two studies can likely be explained by the expression level of ALG-1CD and ALG-2CD proteins achieved with both experimental approaches. Bouasker and Simard's analysis expressed ALG-1 and ALG-2 slicing dead proteins using extrachromosomal arrays, which leads to an important overexpression of the protein. Here, we modified the endogenous loci using the CRISPR-Cas9 gene editing method, which retains the same expression level of endogenous proteins. Thus, this first study with overexpressing conditions likely affects slicing dead ALG-1 and ALG-2 interaction with miRNAs and protein partners, which could cause an imbalance in molecular stoichiometry leading to a potential dominant effect. The mutations of the endogenous loci of *alg-1* and *alg-2* genes performed here prevent causing this effect.

The phenotypical analyses of *alg-1* and *alg-2* catalytically inactive mutant animals demonstrate their contribution to different biological pathways implicating miRNAs, such as fertility, embryogenesis, developmental timing, alae formation, and gonadal arm migration. Interestingly, we observed that the effect on animals varied amongst single and double mutants indicating a different contribution of slicing ALG-1 and ALG-2. As the observed phenotypes are not as penetrant as the ones observed with a complete loss of

either specific miRNA such as let-7 or lin-4 or both *alg-1* and *alg-2* genes (33, 47, 55, 56, 69, 70), it suggests that the slicing Argonautes are not essential for canonical miRNA function and the viability of the worms, at least in normal conditions.

Molecularly, our data indicated that while the slicing activity of ALG-1 and ALG-2 does not affect its association with the GW182 protein, AIN-1 or miRNAs (Figure S6), it does have a significant effect on the level of specific subsets of miRNAs. The limitation of ALG-1 or ALG-2 slicer function to specific cells, tissues, or developmental stages might cause the effect on particular miRNAs. Among the miRNAs misregulated, we cannot find any single one whose misregulation can explain the different phenotypes observed in *alg-1(CD)* and *alg-2*(*CD)* animals. We suggest that the misregulation of several miRNAs could cause the different phenotypes observed in those mutant animals.

In the past, *in vitro* and *in cellulo* approaches have demonstrated that Argonaute slicing activity can help remove the star (or passenger) strand from the miRNA duplex created by Dicer cleavage (26, 45). Consistent with this model, Kotagama *et al* have observed a significant increase of a subset of star miRNAs in *alg-2(CD)* embryo samples. In contrast here, when we monitored the level of guide and star miRNA strand pairs of the significantly dysregulated miRNAs in young adults, despite their low abundance, we observed subsets of miRNA duplexes that appear to accumulate distinctively in *alg-1(CD)* and *alg-2(CD)* animals (Figure S7). However, the variability detected for the miRNA star counts in wild-type samples (likely due to their low abundance) prevents us from assessing any significant effect of Argonaute catalytic activity on the miRNA duplex. Nevertheless, our data could suggest that in young adult animals, both ALG-1 and ALG-2 slicing activity might contribute to duplex cleavage, while in embryos, ALG-2 appears to be the main contributor to this process.

Previous studies in culture cells and *C. elegans* using both ectopically overexpressed slicing dead Argonautes have reported the production of atypical miRNA precursor molecules in absence of catalytically active Argonautes (36, 45). With the approach used here that maintains the endogenous level of both ALG-1 and ALG-2, we did not observe

any aberrant form of miRNA molecules. This suggests that over-expressing slicing dead Argonautes can affect the miRNA processing machinery leading to the production of aberrant molecules. Our data stresses the necessity of performing structure-function studies in experimental conditions in which the molecular stoichiometry of the proteins must be maintained. The recent development of powerful genome editing approaches allows us to design studies to uncover the precise gene function in critical gene regulatory pathways.

Taken together, our study highlights that despite of the maintenance of slicing function in miRNA-specific Argonautes, their physiological and molecular contributions in the canonical miRNA pathway can only been observed for animals exposed to a more stressful environment such as maintaining them at higher temperature. This is further supported when we compare our analyses with Kotagama *et al* who conducted their experiment in less stressful conditions and did not observe any significant phenotypes in animals without miRNA-specific slicing Argonautes. Thus, we can envision that the role of slicing Argonautes is becoming essential in various conditions encountered by the animal in the wild in which components or specific molecular step(s) involved in the release of the miRNA strand from duplexes are becoming less efficient. Future works testing this hypothesis will likely uncover the contribution of diverse underappreciated protein functions such as slicing Argonautes that cannot yet be fully revealed in our well-controlled laboratory conditions.

DATA AVAILABILITY

Raw and processed small RNA-seq datasets have been deposited at NCBI's Gene Expression Omnibus (GEO) repository and are publicly available as of the date of publication. Accession number for the data is GSE222733. This paper does not report original code. All unique and stable reagents and strains generated in this study are available from the lead contact without restriction.

FUNDINGS

This work was supported by The Canadian Institutes of Health Research (CIHR) (M.J.S.) and National Institutes of Health (NIH, GM126458) (A.L.A).

ACKNOWLEDGMENTS

We would like to thank Dr. Katherine McJunkin for sharing data with us prior to publication. We also thank Dr. Weifeng Gu for the help with small RNA analyses, Sarah Côté for technical help, Dr. Zhirong Bao for sharing the *stls10027* transgene strain used for spermatid quantification and Dr. Andrew Singson for providing laboratory resources to complete the sperm quantification. Some strains used in this study are provided by *Caenorhaditis* Genetic Center, which is funded by NIH Office of Research Infrastructure Programs (P40 OD010440). We thank the members of our laboratory for helpful comments. A.P. received a scholarship from Université Laval. V.V. received a scholarship from the Faculty of Medicine of Université Laval and from the Fondation du CHU de Québec. M.L. was a recipient of a scholarship from Natural Sciences and Engineering Research Council of Canada (NSERC). K.A.M. received a NIH Institutional Research and Academic Career Development Award (K12GM093854) Fellowship. M.Q.H. was recipient of scholarship from the Fonds de Recherche du Québec-Santé (FRQ-S).

AUTHOR CONTRIBUTIONS

Conceptualization, A.P. and M.J.S.; Methodology, A.P., V.V., M.L., F.H., K.A.M. M.Q.H., A.L.A. and M.J.S.; Investigation, A.P., V.V., M.L., F.H., K.A.M. and M.Q.H.; Writing – Original Draft, A.P. and M.J.S.; Writing – Review & Editing, A.P., V.V., M.L., F.H., K.A.M. M.Q.H., A.L.A. and M.J.S. Funding Acquisition, M.J.S.; Supervision, A.L.A. and M.J.S.

DECLARATION OF INTEREST

The authors declare no competing interests.

REFERENCES

1. Dexheimer,P.J. and Cochella,L. (2020) MicroRNAs: From Mechanism to Organism. *Front Cell Dev Biol*, **8**.

2. Bartel,D.P. (2018) Metazoan MicroRNAs. *Cell*, **173**, 20–51.

3. Chipman,L.B. and Pasquinelli,A.E. (2019) miRNA Targeting: Growing beyond the Seed. *Trends Genet*, **35**, 215–222.

4. Treiber,T., Treiber,N. and Meister,G. (2019) Regulation of microRNA biogenesis and its crosstalk with other cellular pathways. *Nat Rev Mol Cell Biol*, **20**, 5–20.

5. Nakanishi,K. (2016) Anatomy of <scp>RISC</scp> : how do small <scp>RNAs</scp> and chaperones activate Argonaute proteins? *WIREs RNA*, **7**, 637–660.

6. Sheu-Gruttadauria,J. and MacRae,I.J. (2017) Structural Foundations of RNA Silencing by Argonaute. *J Mol Biol*, **429**, 2619–2639.

7. Medley,J.C., Panzade,G. and Zinovyeva,A.Y. (2021) microRNA strand selection: Unwinding the rules. *Wiley Interdiscip Rev RNA*, **12**.

8. Gebert,L.F.R. and MacRae,I.J. (2019) Regulation of microRNA function in animals. *Nat Rev Mol Cell Biol*, **20**, 21–37.

9. Duchaine,T.F. and Fabian,M.R. (2019) Mechanistic Insights into MicroRNA-Mediated Gene Silencing. *Cold Spring Harb Perspect Biol*, **11**.

10. Jannot,G., Michaud,P., Quévillon Huberdeau,M., Morel-Berryman,L., Brackbill,J.A., Piquet,S., McJunkin,K., Nakanishi,K. and Simard,M.J. (2016) GW182-Free

microRNA Silencing Complex Controls Post-transcriptional Gene Expression during Caenorhabditis elegans Embryogenesis. *PLoS Genet*, **12**, e1006484.

11. Dallaire,A., Frédérick,P.M. and Simard,M.J. (2018) Somatic and Germline MicroRNAs Form Distinct Silencing Complexes to Regulate Their Target mRNAs Differently. *Dev Cell*, **47**, 239-247.e4.

12. Frédérick,P.M. and Simard,M.J. (2022) Regulation and different functions of the animal microRNA-induced silencing complex. *Wiley Interdiscip Rev RNA*, **13**.

13. Swarts,D.C., Jore,M.M., Westra,E.R., Zhu,Y., Janssen,J.H., Snijders,A.P., Wang,Y., Patel,D.J., Berenguer,J., Brouns,S.J.J., *et al.* (2014) DNA-guided DNA interference by a prokaryotic Argonaute. *Nature*, **507**, 258–261.

14. Nakanishi,K. (2022) Anatomy of four human Argonaute proteins. *Nucleic Acids Res*, **50**, 6618–6638.

15. Youngman,E.M. and Claycomb,J.M. (2014) From early lessons to new frontiers: The worm as a treasure trove of small RNA biology. *Front Genet*, **5**, 416.

16. Hutvagner,G. and Simard,M.J. (2008) Argonaute proteins: key players in RNA silencing. *Nature Reviews Molecular Cell Biology 2008 9:1*, **9**, 22–32.

17. Meister,G. (2013) Argonaute proteins: functional insights and emerging roles. *Nat Rev Genet*, **14**, 447–459.

18. Kim,K., Lee,Y.S. and Carthew,R.W. (2007) Conversion of pre-RISC to holo-RISC by Ago2 during assembly of RNAi complexes. *RNA*, **13**, 22–29.

19. Leuschner,P.J.F., Ameres,S.L., Kueng,S. and Martinez,J. (2006) Cleavage of the siRNA passenger strand during RISC assembly in human cells. *EMBO Rep*, **7**, 314–320.

20. Matranga,C., Tomari,Y., Shin,C., Bartel,D.P. and Zamore,P.D. (2005) Passenger-strand cleavage facilitates assembly of siRNA into Ago2-containing RNAi enzyme complexes. *Cell*, **123**, 607–620.

21. Saito,K., Inagaki,S., Mituyama,T., Kawamura,Y., Ono,Y., Sakota,E., Kotani,H., Asai,K., Siomi,H. and Siomi,M.C. (2009) A regulatory circuit for piwi by the large Maf gene traffic jam in Drosophila. *Nature*, **461**, 1296–1299.

22. Reuter,M., Berninger,P., Chuma,S., Shah,H., Hosokawa,M., Funaya,C., Antony,C., Sachidanandam,R. and Pillai,R.S. (2011) Miwi catalysis is required for piRNA amplification-independent LINE1 transposon silencing. *Nature*, **480**, 264–267.

23. de Fazio,S., Bartonicek,N., di Giacomo,M., Abreu-Goodger,C., Sankar,A., Funaya,C., Antony,C., Moreira,P.N., Enright,A.J. and O'carroll,D. (2011) The endonuclease activity of Mili fuels piRNA amplification that silences LINE1 elements. *Nature*, **480**, 259–263.

24. Bagijn,M.P., Goldstein,L.D., Sapetschnig,A., Weick,E.M., Bouasker,S., Lehrbach,N.J., Simard,M.J. and Miska,E.A. (2012) Function, targets, and evolution of Caenorhabditis elegans piRNAs. *Science*, **337**, 574–578.

25. Tolia,N.H. and Joshua-Tor,L. (2007) Slicer and the argonautes. *Nat Chem Biol*, **3**, 36–43.

26. Jee,D., Yang,J.S., Park,S.M., Farmer,D.T., Wen,J., Chou,T., Chow,A., McManus,M.T., Kharas,M.G. and Lai,E.C. (2018) Dual Strategies for Argonaute2-Mediated Biogenesis of Erythroid miRNAs Underlie Conserved Requirements for Slicing in Mammals. *Mol Cell*, **69**, 265-278.e6.

27. Cheloufi,S., dos Santos,C.O., Chong,M.M.W. and Hannon,G.J. (2010) A dicer-independent miRNA biogenesis pathway that requires Ago catalysis. *Nature*, **465**, 584–589.

28. Cifuentes,D., Xue,H., Taylor,D.W., Patnode,H., Mishima,Y., Cheloufi,S., Ma,E., Mane,S., Hannon,G.J., Lawson,N.D., *et al.* (2010) A novel miRNA processing pathway independent of Dicer requires Argonaute2 catalytic activity. *Science*, **328**, 1694–1698.

29. Yang,S., Maurin,T., Robine,N., Rasmussen,K.D., Jeffrey,K.L., Chandwani,R., Papapetrou,E.P., Sadelain,M., O'Carroll,D. and Lai,E.C. (2010) Conserved

vertebrate mir-451 provides a platform for Dicer-independent, Ago2-mediated microRNA biogenesis. *Proc Natl Acad Sci U S A*, **107**, 15163–15168.

30. Meister,G., Landthaler,M., Patkaniowska,A., Dorsett,Y., Teng,G. and Tuschl,T. (2004) Human Argonaute2 mediates RNA cleavage targeted by miRNAs and siRNAs. *Mol Cell*, **15**, 185–197.

31. Liu,J., Carmell,M.A., Rivas,F. v., Marsden,C.G., Thomson,J.M., Song,J.J., Hammond,S.M., Joshua-Tor,L. and Hannon,G.J. (2004) Argonaute2 is the catalytic engine of mammalian RNAi. *Science*, **305**, 1437–1441.

32. Park,M.S., Phan,H.D., Busch,F., Hinckley,S.H., Brackbill,J.A., Wysocki,V.H. and Nakanishi,K. (2017) Human Argonaute3 has slicer activity. *Nucleic Acids Res*, **45**, 11867–11877.

33. Grishok,A., Pasquinelli,A.E., Conte,D., Li,N., Parrish,S., Ha,I., Baillie,D.L., Fire,A., Ruvkun,G. and Mello,C.C. (2001) Genes and mechanisms related to RNA interference regulate expression of the small temporal RNAs that control C. elegans developmental timing. *Cell*, **106**, 23–34.

34. Yigit,E., Batista,P.J., Bei,Y., Pang,K.M., Chen,C.C.G., Tolia,N.H., Joshua-Tor,L., Mitani,S., Simard,M.J. and Mello,C.C. (2006) Analysis of the C. elegans Argonaute family reveals that distinct Argonautes act sequentially during RNAi. *Cell*, **127**, 747–757.

35. Brown,K.C., Svendsen,J.M., Tucci,R.M., Montgomery,B.E. and Montgomery,T.A. (2017) ALG-5 is a miRNA-associated Argonaute required for proper developmental timing in the Caenorhabditis elegans germline. *Nucleic Acids Res*, **45**, 9093–9107.

36. Bouasker,S. and Simard,M.J. (2012) The slicing activity of miRNA-specific Argonautes is essential for the miRNA pathway in C. elegans. *Nucleic Acids Res*, **40**, 10452–10462.

37. Brenner,S. (1974) The genetics of Caenorhabditis elegans. *Genetics*, **77**, 71–94.

38. Ghanta,K.S., Ishidate,T. and Mello,C.C. (2021) Microinjection for precision genome editing in Caenorhabditis elegans. *STAR Protoc*, **2**.

39. Huang,J., Wang,H., Chen,Y., Wang,X. and Zhang,H. (2012) Residual body removal during spermatogenesis in C. elegans requires genes that mediate cell corpse clearance. *Development*, **139**, 4613–4622.

40. Maniates,K.A., Olson,B.S. and Abbott,A.L. (2021) Sperm fate is promoted by the mir-44 microRNA family in the Caenorhabditis elegans hermaphrodite germline. *Genetics*, **217**.

41. Langmead,B., Trapnell,C., Pop,M. and Salzberg,S.L. (2009) Ultrafast and memory-efficient alignment of short DNA sequences to the human genome. *Genome Biol*, **10**.

42. Jurka,J., Kapitonov,V. v., Pavlicek,A., Klonowski,P., Kohany,O. and Walichiewicz,J. (2005) Repbase Update, a database of eukaryotic repetitive elements. *Cytogenet Genome Res*, **110**, 462–467.

43. Kozomara,A. and Griffiths-Jones,S. (2011) miRBase: integrating microRNA annotation and deep-sequencing data. *Nucleic Acids Res*, **39**.

44. Stein,L.D., Mungall,C., Shu,S., Caudy,M., Mangone,M., Day,A., Nickerson,E., Stajich,J.E., Harris,T.W., Arva,A., *et al.* (2002) The generic genome browser: a building block for a model organism system database. *Genome Res*, **12**, 1599–1610.

45. Diederichs,S. and Haber,D.A. (2007) Dual role for argonautes in microRNA processing and posttranscriptional regulation of microRNA expression. *Cell*, **131**, 1097–1108.

46. Tops,B.B.J., Plasterk,R.H.A. and Ketting,R.F. (2006) The Caenorhabditis elegans Argonautes ALG-1 and ALG-2: almost identical yet different. *Cold Spring Harb Symp Quant Biol*, **71**, 189–194.

47. Vasquez-Rifo,A., Jannot,G., Armisen,J., Labouesse,M., Bukhari,S.I.A., Rondeau,E.L., Miska,E.A. and Simard,M.J. (2012) Developmental characterization of the microRNA-specific C. elegans Argonautes alg-1 and alg-2. *PLoS One*, **7**.

48. Bukhari,S.I.A., Vasquez-Rifo,A., Gagné,D., Paquet,E.R., Zetka,M., Robert,C., Masson,J.Y. and Simard,M.J. (2012) The microRNA pathway controls germ cell proliferation and differentiation in C. elegans. *Cell Res*, **22**, 1034–1045.

49. Begasse,M.L., Leaver,M., Vazquez,F., Grill,S.W. and Hyman,A.A. (2015) Temperature Dependence of Cell Division Timing Accounts for a Shift in the Thermal Limits of C. elegans and C. briggsae. *Cell Rep*, **10**, 647–653.

50. Servello,F.A., Fernandes,R., Eder,M., Harris,N., Martin,O.M., Oswal,N., Lindberg,A., Derosiers,N., Sengupta,P., Stroustrup,N., *et al.* (2022) Neuronal temperature perception induces specific defenses that enable C. elegans to cope with the enhanced reactivity of hydrogen peroxide at high temperature. *Elife*, **11**.

51. Michaud,P., Shah,V.N., Adjibade,P., Houle,F., Huberdeau,M.Q., Rioux,R., Lavoie-Ouellet,C., Gu,W., Mazroui,R. and Simard,M.J. (2021) The RabGAP TBC-11 controls Argonaute localization for proper microRNA function in C. elegans. *PLoS Genet*, **17**.

52. Hammell,C.M., Lubin,I., Boag,P.R., Blackwell,T.K. and Ambros,V. (2009) nhl-2 Modulates microRNA activity in Caenorhabditis elegans. *Cell*, **136**, 926–938.

53. Quévillon Huberdeau,M., Shah,V.N., Nahar,S., Neumeier,J., Houle,F., Bruckmann,A., Gypas,F., Nakanishi,K., Großhans,H., Meister,G., *et al.* (2022) A specific type of Argonaute phosphorylation regulates binding to microRNAs during C. elegans development. *Cell Rep*, **41**, 111822.

54. Alessi,A.F., Khivansara,V., Han,T., Freeberg,M.A., Moresco,J.J., Tu,P.G., Montoye,E., Yates,J.R., Karp,X. and Kim,J.K. (2015) Casein kinase II promotes target silencing by miRISC through direct phosphorylation of the DEAD-box RNA helicase CGH-1. *Proc Natl Acad Sci U S A*, **112**, E7213–E7222.

55. Lee,R.C., Feinbaum,R.L. and Ambros,V. (1993) The C. elegans heterochronic gene lin-4 encodes small RNAs with antisense complementarity to lin-14. *Cell*, **75**, 843–854.

56. Reinhart,B.J., Slack,F.J., Basson,M., Pasquienelll,A.E., Bettlnger,J.C., Rougvle,A.E., Horvitz,H.R. and Ruvkun,G. (2000) The 21-nucleotide let-7 RNA regulates developmental timing in Caenorhabditis elegans. *Nature*, **403**, 901–906.

57. Abbott,A.L., Alvarez-Saavedra,E., Miska,E.A., Lau,N.C., Bartel,D.P., Horvitz,H.R. and Ambros,V. (2005) The let-7 MicroRNA family members mir-48, mir-84, and mir-241 function together to regulate developmental timing in Caenorhabditis elegans. *Dev Cell*, **9**, 403–414.

58. Brenner,J.L., Jasiewicz,K.L., Fahley,A.F., Kemp,B.J. and Abbott,A.L. (2010) Loss of individual microRNAs causes mutant phenotypes in sensitized genetic backgrounds in C. elegans. *Curr Biol*, **20**, 1321–1325.

59. Burke,S.L., Hammell,M. and Ambros,V. (2015) Robust Distal Tip Cell Pathfinding in the Face of Temperature Stress Is Ensured by Two Conserved microRNAS in Caenorhabditis elegans. *Genetics*, **200**, 1201–1218.

60. Aalto,A.P., Nicastro,I.A., Broughton,J.P., Chipman,L.B., Schreiner,W.P., Chen,J.S. and Pasquinelli,A.E. (2018) Opposing roles of microRNA Argonautes during Caenorhabditis elegans aging. *PLoS Genet*, **14**.

61. Kato,M., Chen,X., Inukai,S., Zhao,H. and Slack,F.J. (2011) Age-associated changes in expression of small, noncoding RNAs, including microRNAs, in C. elegans. *RNA*, **17**, 1804–1820.

62. Boehm,M. and Slack,F. (2005) A developmental timing microRNA and its target regulate life span in C. elegans. *Science*, **310**, 1954–1957.

63. de Lencastre,A., Pincus,Z., Zhou,K., Kato,M., Lee,S.S. and Slack,F.J. (2010) MicroRNAs both promote and antagonize longevity in C. elegans. *Curr Biol*, **20**, 2159–2168.

64. Ibáñez-Ventoso,C., Yang,M., Guo,S., Robins,H., Padgett,R.W. and Driscoll,M. (2006) Modulated microRNA expression during adult lifespan in Caenorhabditis elegans. *Aging Cell*, **5**, 235–246.

65. Zhu,C., Ji,C.B., Zhang,C.M., Gao,C.L., Zhu,J.G., Qin,D.N., Kou,C.Z., Zhu,G.Z., Shi,C.M. and Guo,X.R. (2010) The lin-4 gene controls fat accumulation and longevity in Caenorhabditis elegans. *Int J Mol Sci*, **11**, 4814–4825.

66. Pincus,Z., Smith-Vikos,T. and Slack,F.J. (2011) MicroRNA predictors of longevity in Caenorhabditis elegans. *PLoS Genet*, **7**.

67. Boulias,K. and Horvitz,H.R. (2012) The C. elegans microRNA mir-71 acts in neurons to promote germline-mediated longevity through regulation of DAF-16/FOXO. *Cell Metab*, **15**, 439–450.

68. Smith-Vikos,T., de Lencastre,A., Inukai,S., Shlomchik,M., Holtrup,B. and Slack,F.J. (2014) MicroRNAs mediate dietary-restriction-induced longevity through PHA-4/FOXA and SKN-1/Nrf transcription factors. *Curr Biol*, **24**, 2238–2246.

69. Ecsedi,M., Rausch,M. and Großhans,H. (2015) The let-7 microRNA directs vulval development through a single target. *Dev Cell*, **32**, 335–344.

70. Slack,F.J., Basson,M., Liu,Z., Ambros,V., Horvitz,H.R. and Ruvkun,G. (2000) The lin-41 RBCC gene acts in the C. elegans heterochronic pathway between the let-7 regulatory RNA and the LIN-29 transcription factor. *Mol Cell*, **5**, 659–669.

FIGURES LEGEND

Figure 1. Catalytically dead ALG-1 and ALG-2 affect animal fitness. (A) The alignment of ALG-1/2/5, done on CLUSTAL O (1.2.4) showing the presence and absence of catalytic tetrad (the four amino acids DEDH are identified by the red rectangles). **(B)** Schematic representation of the four Argonaute domains (N-terminal, PAZ, MID and PIWI), the catalytic tetrad of ALG-1 and ALG-2 and generated catalytic dead endogenous Argonaute (ALG-1/2) mutants by CRISPR-Cas9 system. (schematic diagram was created using Biorender). **(C,D)** The worm fitness was observed under normal table top microscope at two different temperatures: 20°C (panel **C**) and 25°C (panel **D**). The percentage of sick (represented by pleiotropic phenotypes such as developmental arrest, protruding vulva, egg laying defect) and dead (larval death, burst) worms are indicated. The number of animals scored (*n*) is indicated. *P* value was obtained by two tailed Fisher's exact test (**p*<0.05, ***p*<0.01, ****p*<0.001, *****p*<0.0001). **(E)** Total hatched larvae were

counted for P0 mothers of each genotype. The box plot indicates the minimum and maximum brood size as well as mean per genotype. The number of animals scored (*n*) is indicated. *P* value was counted using Kolmogorov test (**p*<0.05, ***p*<0.01, ****p*<0.001, *****p*<0.0001) to include the extreme data points.

Figure 2. ALG-1 and ALG-2 catalytic activity contributed to the miRNA pathway. (A) Alae defects and **(B)** gonadal arm migration defects in young adult animals, were scored under DIC Nomarski microscopy. The number of animals scored (*n*) is indicated. *P* value was obtained by two tailed Fisher's exact test (**p*<0.05, ***p*<0.01, ****p*<0.001, *****p*<0.0001). Right side panels show representative images of defect observed on affected animals. The scale bars on alae and gonadal arm migration indicate 10µm and 20µm, respectively.

Figure 3. The role of slicer activity of ALG-1 and ALG-2 on animal lifespan. (A-G) Survival curve shows the lifespan of wild-type and ALG-1 and ALG-2 mutants. Lifespan assays were carried out with a population of $n \geq 37$ animals for each genotype. *P* value was obtained by Gehan-Breslow-Wilcoxon method (**p*<0.05, ***p*<0.01, ****p*<0.001, *****p*<0.0001)

Figure 4. The loss of ALG-1 and ALG-2 slicing activity causes dysregulation in overall miRNA expression in young adults. Heatmap depicting the degree of similarity of each sample and their genotype based on the overall miRNA guide strand expression in young adults. *alg-1(CD)* and *alg-1(CD);alg-2(CD)* genotypes cluster together indicating their similarity towards each other and cluster away from *alg-2(CD)* and WT, indicating their dissimilarity towards the other two genotypes. The tile color represents the number of standard deviations above (Red) or below (Blue) the mean expression of a miRNA (Known as Z-Score). Agglomerative hierarchical clustering based on Euclidean distance is performed on the samples (columns) and miRNA (rows), which is represented by their respective dendrograms.

Figure 5. Catalytically dead ALG-1 and 2 Argonautes have significant and contrasting impact on the clusters of miRNAs. (A) Heatmap of the various clusters of significantly dysregulated miRNA (guide strand) in mutants compared to WT (2-3 replicates per strain). The tile color represents the number of standard deviations above (Red) or below (Blue) the mean expression of a miRNA (Known as Z-Score). Agglomerative hierarchical clustering based on Euclidean distance is performed on the samples (columns) and miRNA (rows), which is represented by their respective dendrograms. **(B)** Venn diagram depicting the significant up regulated miRNAs (guide strands) in *alg-1 (CD)* (light green), *alg-2(CD)* (light orange), *alg-1(CD); alg-2*(CD) (light blue) compared to WT. **(C)** Venn diagram depicting the significant down regulated miRNAs (guide strands) in *alg-1 (CD)* (light green), *alg-2(CD)* (light orange), *alg-1(CD); alg-2*(CD) (light blue) compared to WT.

A

```
ALG-5    ····CVRSQNVSKASPHTLSNLCMKINSKLGGINVILSS-PPQSLNSEPVLFIGCHLTRSSLAS 660
ALG-1    ····CVQAKNAIRTTPQTLSNLCLKMNVKLGGVNSILLPNVRPRIFNEPVIFFGCDITHPPAGD 769
ALG-2    ····CVQAKNAIRTTPQTLSNLCLKMNVKLGGVNSILLPNVRPRIFNEPVIFLGCDITHPAAGD 654

ALG-5     SSDSTSSIAHCDSSIACLVGSMDGHPTQFSPIFRTQPRHQRTIVDMCEMTREAIINFRKS 720
ALG-1     S---------RKPSIAAVVGSMDAHPSRYAATVRVQQHRQEIISDLTYMVRELLVQFYRN 820
ALG-2     T---------RKPSIAAVVGSMDAHPSRYAATVRVQQHRQEIITDLTYMVRELLVQFYRN 705

ALG-5    TGFKPHKIIIYRAGIADVTVDEIMQTELRAVRDACAMIEYGFQPGITFIGLDVTHHTRLF 780
ALG-1    TRFKPARIVVYRDGVSEGQFFNVLQYELRAIREACMMLERGYQPGITFIAVQKRHHTRLF 880
ALG-2    TRFKPARIVVYRDGVSEGQLFNVLQYELRAIREACVMLESGYQPGITFIAVQKRHHTRLF 765

ALG-5    ···· ADIHEMTYQLCHTQSRCTRSVSIPSPVYYAKLVAQRAKILMADENFDMERFRL--CGIGR 898····
ALG-1    ···· DELQQLTYQMCHTYVRCTRSVSIPAPAYYAHLVAFRARYHLVDREHDSGE-GSQPSGT-S 998····
ALG-2    ···· DELQQLTYQMCHTYVRCTRSVSIPAPAYYAHLVAFRARYHLVDRDHGSGEEGSQPSGTSS 885····
```

B

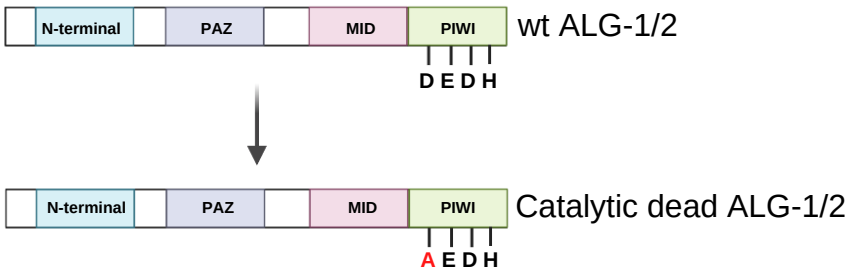

C

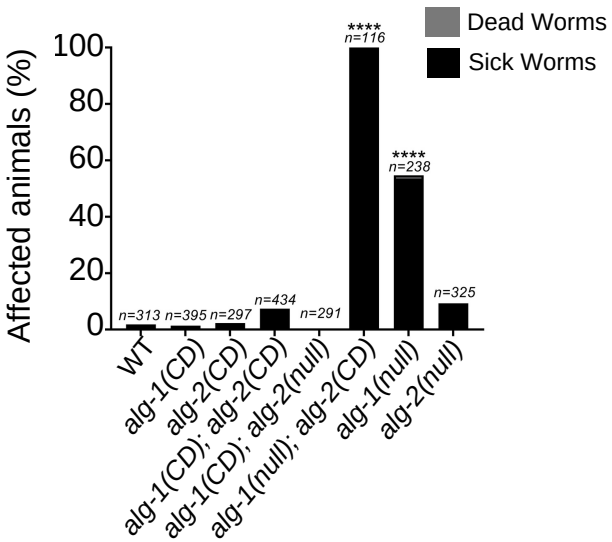

D

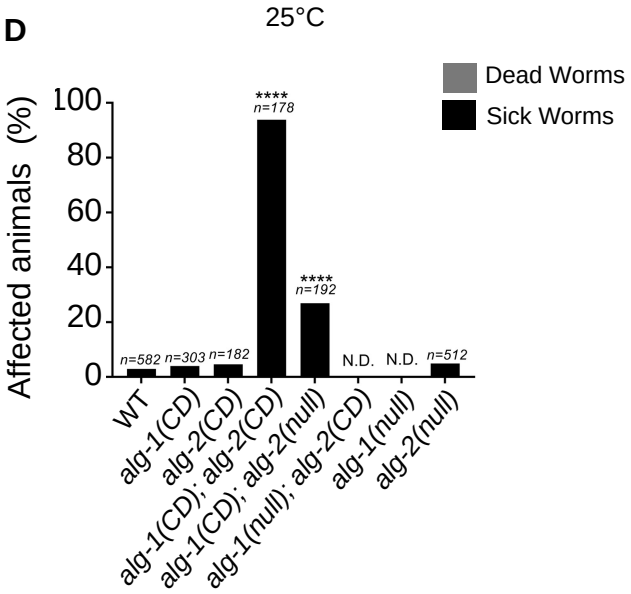

E

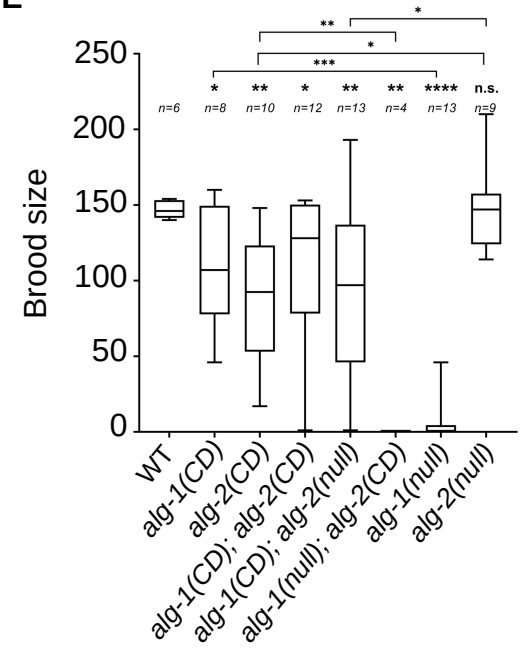

Figure 1

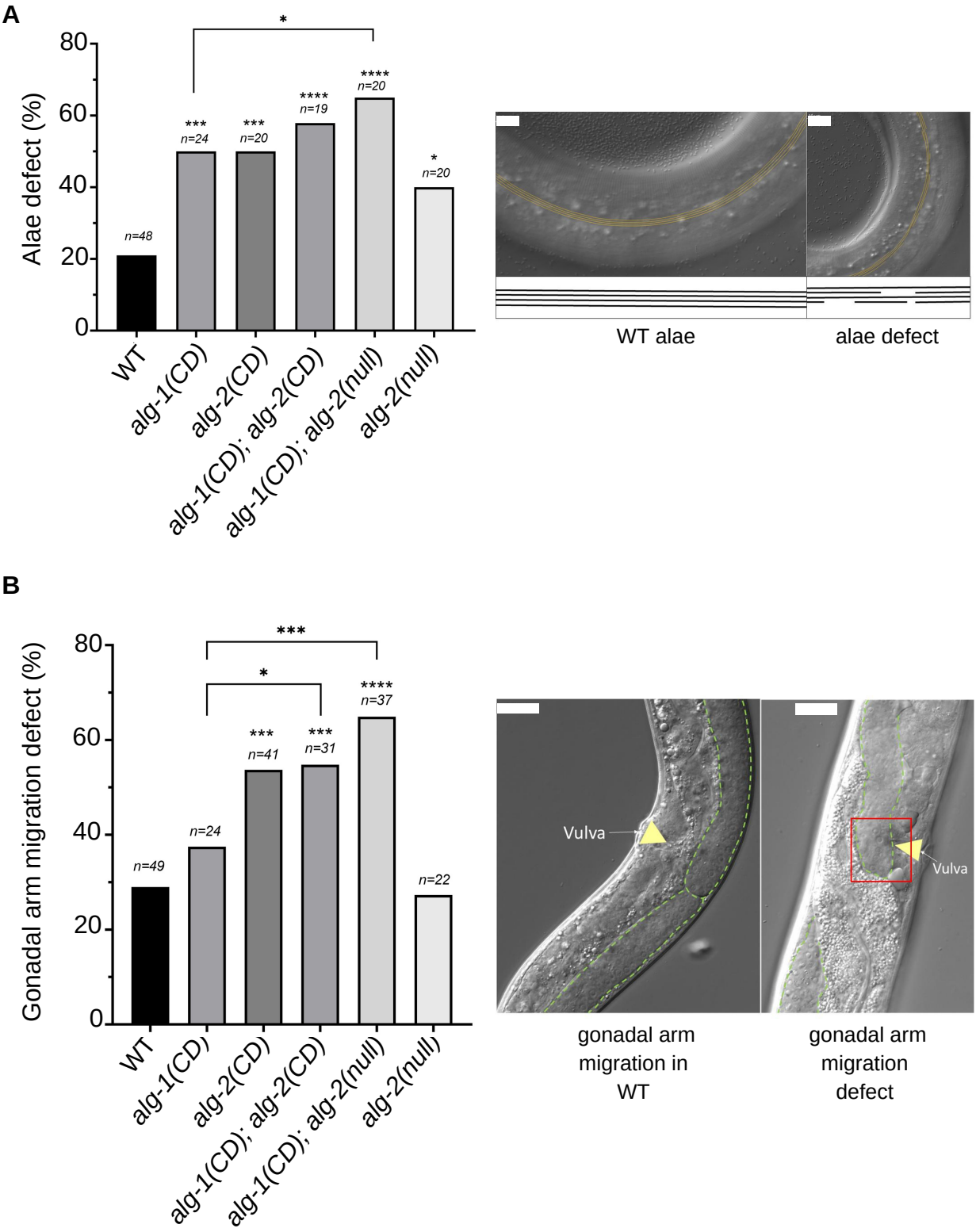
A
Alae defect (%)
80
60
40
20
0
*
***
n=24
***
n=20
****
n=19
****
n=20
*
n=20
n=48
WT
alg-1(CD)
alg-2(CD)
alg-1(CD); alg-2(CD)
alg-1(CD); alg-2(null)
alg-2(null)
WT alae
alae defect
B
Gonadal arm migration defect (%)
80
60
40
20
0
***
*
***
n=41
***
n=31
****
n=37
n=49
n=24
n=22
WT
alg-1(CD)
alg-2(CD)
alg-1(CD); alg-2(CD)
alg-1(CD); alg-2(null)
alg-2(null)
Vulva
Vulva
gonadal arm migration in WT
gonadal arm migration defect

Figure 2

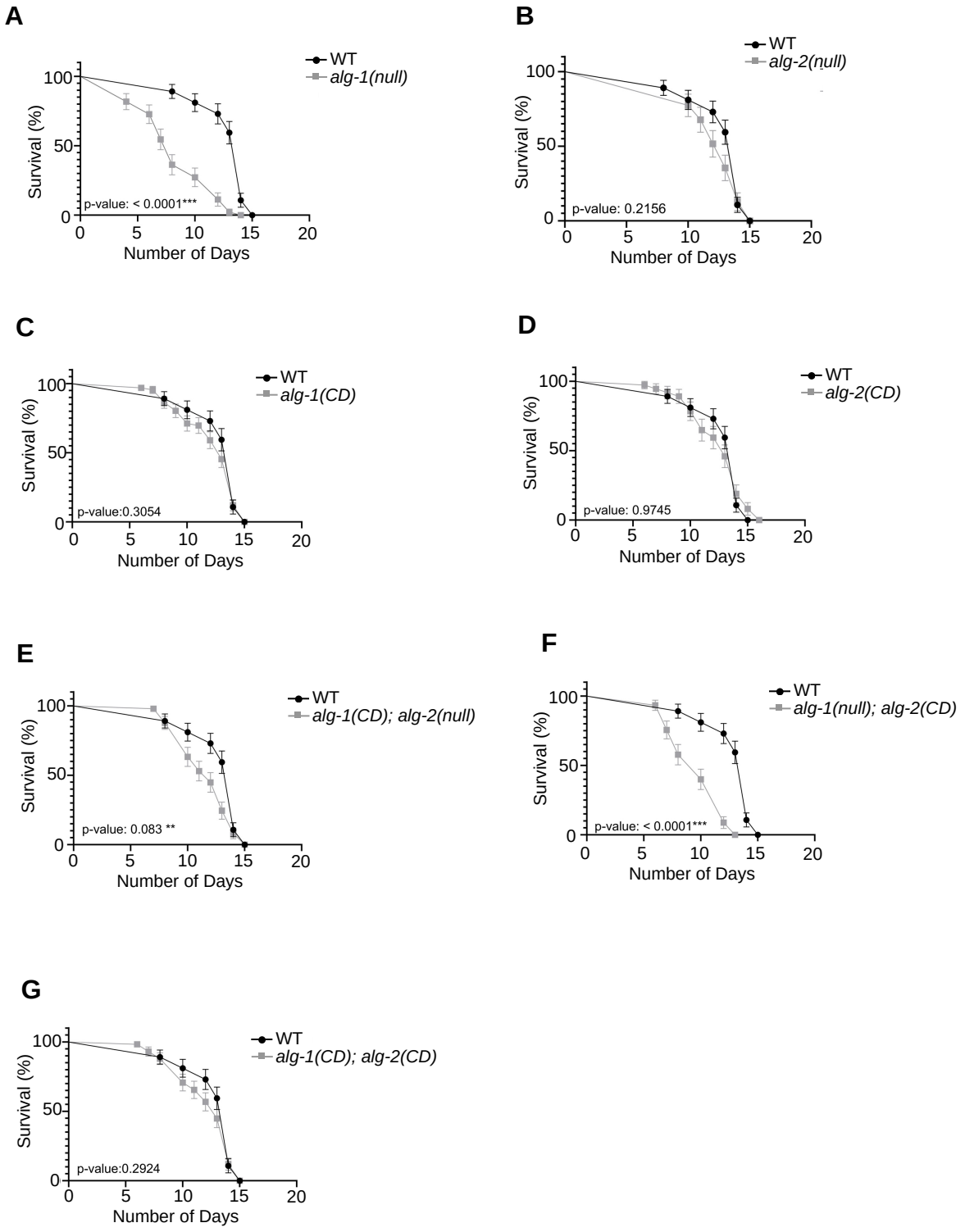
A
WT
alg-1(null)
Survival (%)
Number of Days
p-value: < 0.0001***
B
WT
alg-2(null)
Survival (%)
Number of Days
p-value: 0.2156
C
WT
alg-1(CD)
Survival (%)
Number of Days
p-value:0.3054
D
WT
alg-2(CD)
Survival (%)
Number of Days
p-value: 0.9745
E
WT
alg-1(CD); alg-2(null)
Survival (%)
Number of Days
p-value: 0.083 **
F
WT
alg-1(null); alg-2(CD)
Survival (%)
Number of Days
p-value: < 0.0001***
G
WT
alg-1(CD); alg-2(CD)
Survival (%)
Number of Days
p-value:0.2924

Figure 3

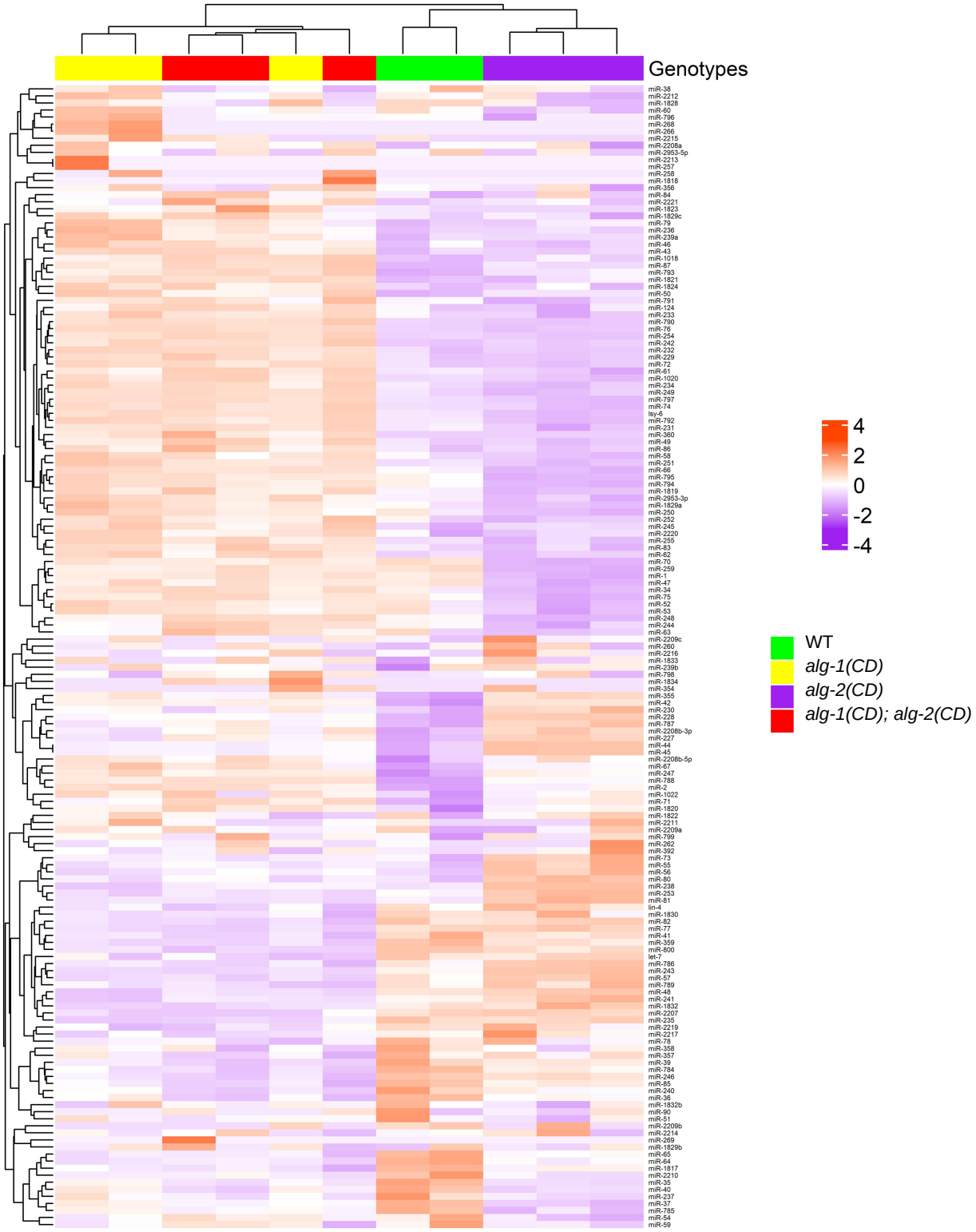

Figure 4

A

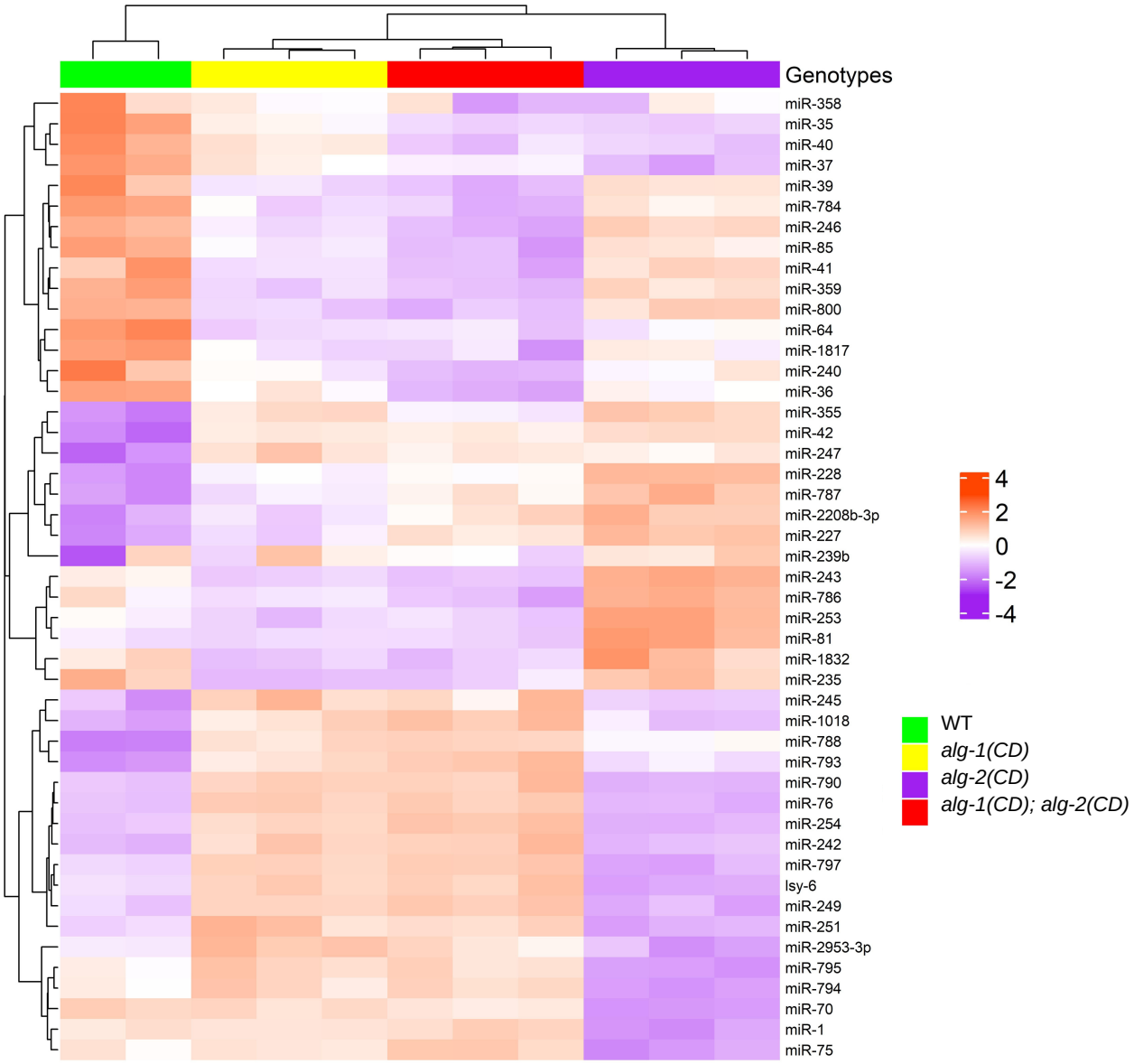
Genotypes
miR-358
miR-35
miR-40
miR-37
miR-39
miR-784
miR-246
miR-85
miR-41
miR-359
miR-800
miR-64
miR-1817
miR-240
miR-36
miR-355
miR-42
miR-247
miR-228
miR-787
miR-2208b-3p
miR-227
miR-239b
miR-243
miR-786
miR-253
miR-81
miR-1832
miR-235
miR-245
miR-1018
miR-788
miR-793
miR-790
miR-76
miR-254
miR-242
miR-797
lsy-6
miR-249
miR-251
miR-2953-3p
miR-795
miR-794
miR-70
miR-1
miR-75
4
2
0
-2
-4
WT
alg-1(CD)
alg-2(CD)
alg-1(CD); alg-2(CD)

Figure 5

B

Significantly Up-regulated miRNAs in mutants compared to WT

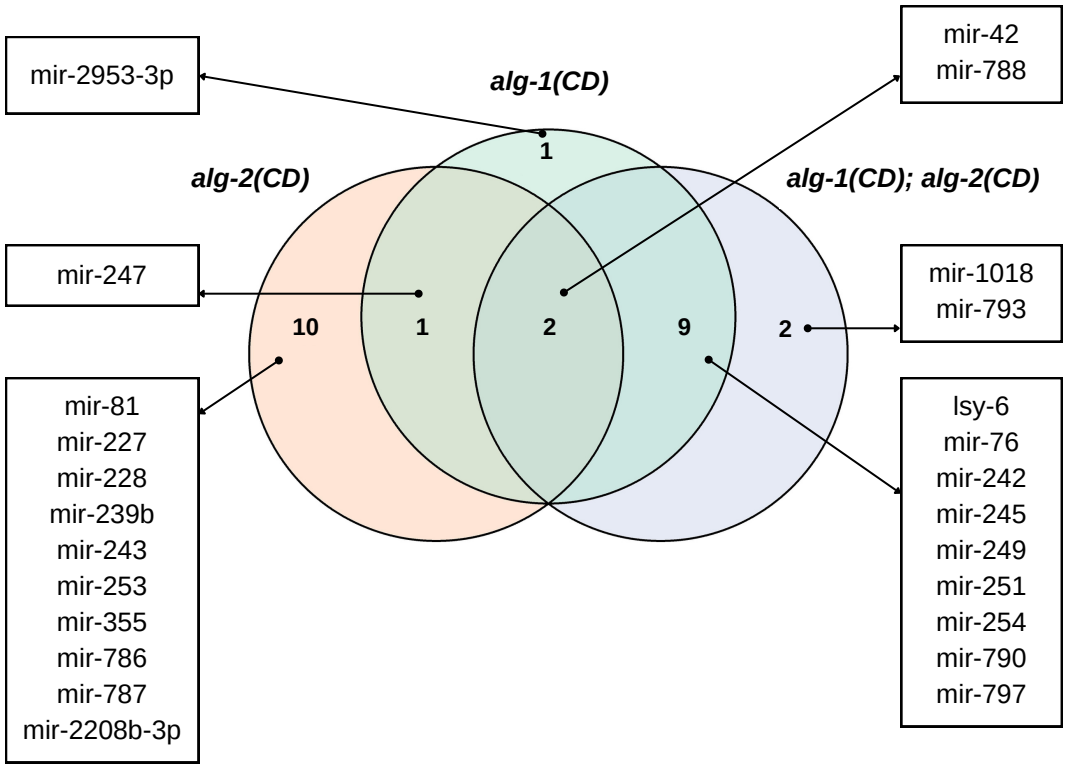

C

Significantly Down-regulated miRNAs in mutants compared to WT

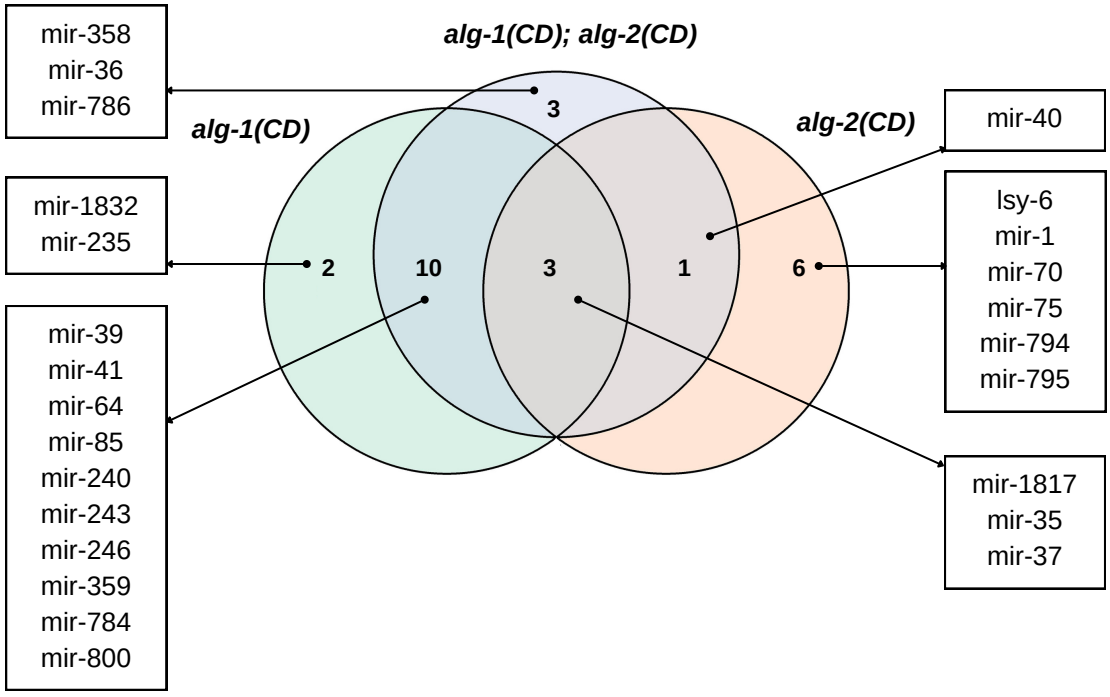

Figure 5

Defining the contribution of microRNA-specific slicing Argonautes in animals

Anisha Pal, Vaishnav Vasudevan, François Houle, Michael Lantin, Katherine A. Maniates, Miguel Quévillon Huberdeau, Allison L. Abbott, Martin J. Simard

SUPPLEMENTAL FIGURES LEGEND

Figure S1. Steady state level of ALG-1 and ALG-2. Western blot shows the stability of ALG-1(CD) and endogenously FLAG tagged ALG-2(CD) compared to ALG-1 and FLAG::ALG-2 in presence of 100μM proteasome inhibitor (MG132) in young adults (**A**,**B**). The images represent one of the blots of three replicates.

Figure S2. The effect of ALG-1 and ALG-2 catalytic activity on fertility. (A) Quantification of sperm, present in catalytic argonaute mutants in specific background. Mean along with SEM for each genotype are shown. The sperm are counted from *n*=10 worms for each genotype. One-way anova followed by Tukey's multiple comparison test was done to find out the significance between multiple genotypes. **(B)** Percentage of unfertilised oocyte was counted after putting 4 young adults per plate (*n*=5) and monitored for 48 hrs. The *P*-value were obtained by two tailed t-test. **(C)** Representative images of different phenotypes, observed.

Figure S3. Correlation among the samples and genotypes based on the mature miRNA population. (A) Correlation performed using all 162 expressed miRNA guide strands with the spearman correlation coefficient (ρ) reported for each sample correlation with another. *alg-1(CD)* positively correlates to *alg-1(CD);alg-2(CD)* with a correlation value ranging from 0.38 to 0.55 **(B)** Correlation performed using 47 significantly dysregulated miRNA guide strands with the spearman correlation coefficient (ρ) reported

for each samples correlation with another. *alg-1(CD)* shows increased positive correlation to *alg-1(CD);alg-2(CD)* with value ranging from 0.53 to 0.82

Figure S4. The effect of ALG-1 and 2 catalytic activities on miRNA passenger strand level. (A) Heatmap depicting the overall abundance of miRNA passenger strands in young adults in mentioned genotype. **(B)** Heatmap shows the clusters of significantly dysregulated miRNA (passenger strand) in mutants compared to wild-type young adult animals (2-3 replicates per strain). (**A-B**) The tile color represents the number of standard deviations above (Red) or below (Blue) the mean expression of a miRNA (Known as Z-Score). Agglomerative hierarchical clustering based on Euclidean distance is performed on the samples (columns) and miRNA (rows), which is represented by their respective dendrograms.

Figure S5. Altering the catalytic activity of ALG-1 and ALG-2 does not influence the production of miRNAs. Both guide and star strands miRNAs were detected in young adults after total RNA extraction, followed by Northern blot. Complementary probes were used to detect specific miRNA strands (Table S5). SL1 RNA was probed and used as loading control.

Figure S6. The loss of ALG-1 and ALG-2 catalytic activity does not affect their interaction with GW182 protein AIN-1 and miRNAs. (A) Western blot of AIN-1 after ALG-1 immunoprecipitation from total protein extracts prepared with *alg-1(CD)* and wild-type embryos. **(B)** Western blot of AIN-1 after Flag::ALG-2 immunoprecipitation from total protein extracts prepared with *flag::alg-2(CD)* and *flag::alg-2* embryos. (**A-B**) Input is shown in the left panels and Actin is shown as a loading control. The images are representative of three replicates. **(C)** Boxplot of log2 Normalised Reads per million of detected guide miRNAs in ALG-1 (green) and FLAG::ALG-2 (red) immunoprecipitated complexes. There is no difference in the overall abundance of miRNAs associated to ALG-1(CD) or ALG-2(CD) when compared to the abundance of miRNAs associated to their respective wild-type counterparts.

Figure S7. Effect of the slicing activity of ALG-1 and ALG-2 on guide and star miRNA pairs. Heatmap depicting abundance of guide and star strand miRNAs (pair) found to be significantly upregulated (guide and/or star strands) in either *alg-1(CD)* or *alg-2(CD)* mutant animals when compared to wild-type animals. The heatmap is split into two blocks based on the miRNAs and mutant specific upregulation and clustered by samples to verify for similarity among samples and genotypes for these specific guide and star pairs. The tile color represents the number of standard deviations above (Red) or below (Blue) the mean expression of a miRNA (Known as Z-Score). Agglomerative hierarchical clustering based on Euclidean distance is performed on the samples (columns) and miRNA (rows), which is represented by their respective dendrograms.

SUPPLEMENTARY TABLES (EXCEL FILE)

Table S1: Oligonucleotides used for this study

Table S2-S4: The details of CRISPR mutants, generated in this study

Table S5: Strains used in this study

Table S6: Probes used for Northern Blot

Table S7: Young adult samples used for sequencing

Table S8: Embryos samples used for sequencing

Table S9: Normalised Reads Per Million of all young adult samples

Table S10: Normalised Reads Per Million of all embryos samples

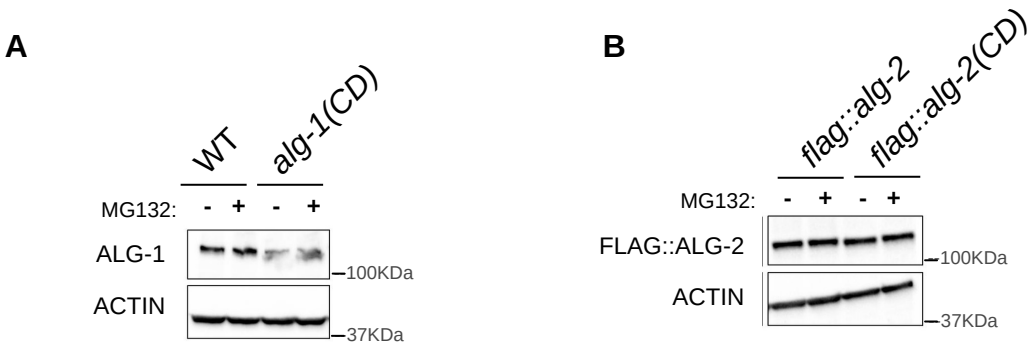
A
WT
alg-1(CD)
MG132:
- + - +
ALG-1
100KDa
ACTIN
37KDa
B
flag::alg-2
flag::alg-2(CD)
MG132:
- + - +
FLAG::ALG-2
100KDa
ACTIN
37KDa

Figure S1

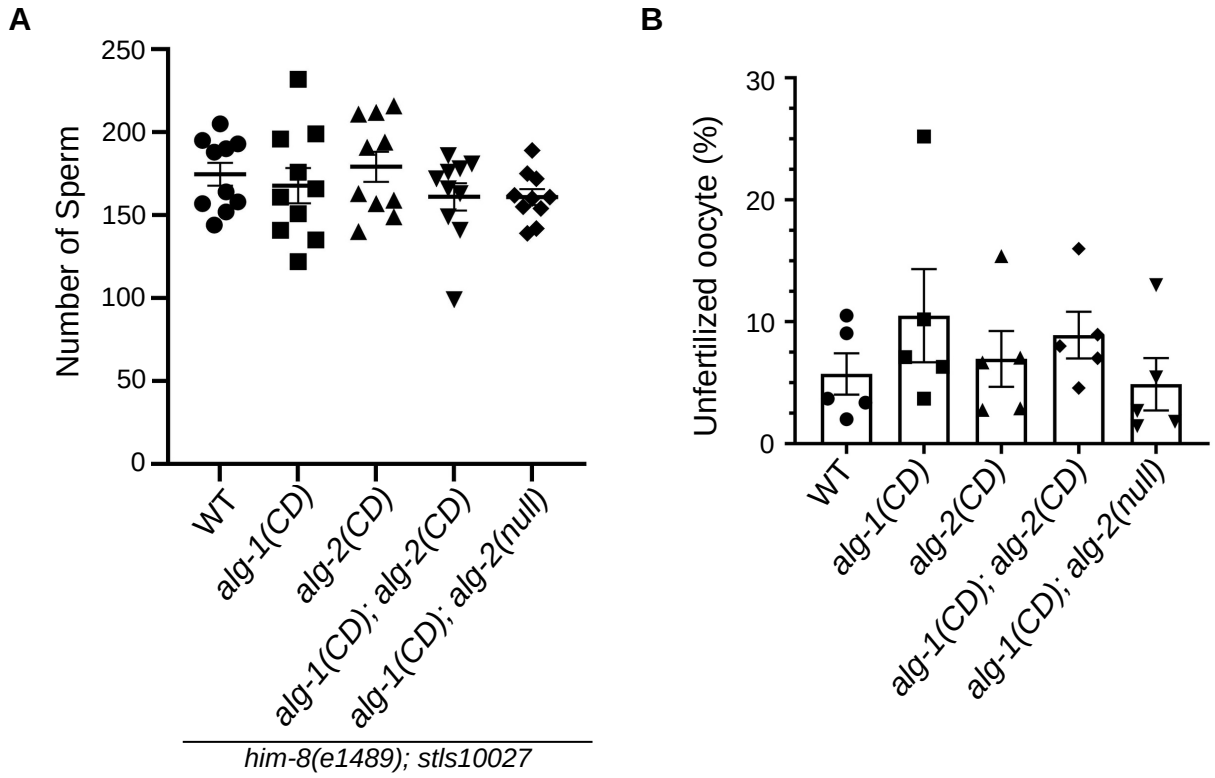
A
Number of Sperm
250
200
150
100
50
0
WT
alg-1(CD)
alg-2(CD)
alg-1(CD); alg-2(CD)
alg-1(CD); alg-2(null)
him-8(e1489); stls10027
B
Unfertilized oocyte (%)
30
20
10
0
WT
alg-1(CD)
alg-2(CD)
alg-1(CD); alg-2(CD)
alg-1(CD); alg-2(null)

Figure S2

A

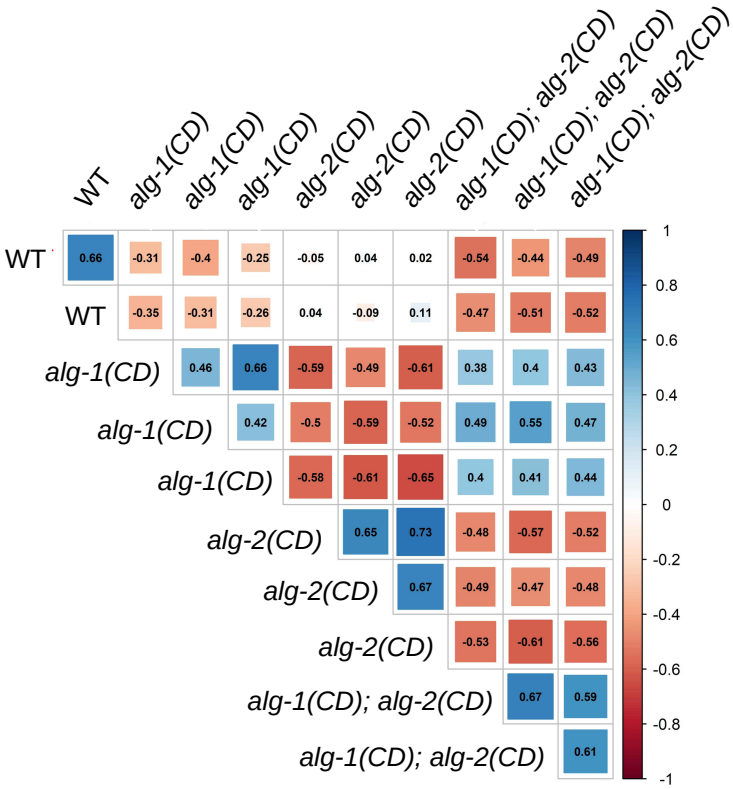
WT
alg-1(CD)
alg-1(CD)
alg-1(CD)
alg-2(CD)
alg-2(CD)
alg-2(CD)
alg-1(CD); alg-2(CD)
alg-1(CD); alg-2(CD)
alg-1(CD); alg-2(CD)
WT 0.66 -0.31 -0.4 -0.25 -0.05 0.04 0.02 -0.54 -0.44 -0.49
WT -0.35 -0.31 -0.26 0.04 -0.09 0.11 -0.47 -0.51 -0.52
alg-1(CD) 0.46 0.66 -0.59 -0.49 -0.61 0.38 0.4 0.43
alg-1(CD) 0.42 -0.5 -0.59 -0.52 0.49 0.55 0.47
alg-1(CD) -0.58 -0.61 -0.65 0.4 0.41 0.44
alg-2(CD) 0.65 0.73 -0.48 -0.57 -0.52
alg-2(CD) 0.67 -0.49 -0.47 -0.48
alg-2(CD) -0.53 -0.61 -0.56
alg-1(CD); alg-2(CD) 0.67 0.59
alg-1(CD); alg-2(CD) 0.61
1
0.8
0.6
0.4
0.2
0
-0.2
-0.4
-0.6
-0.8
-1

B

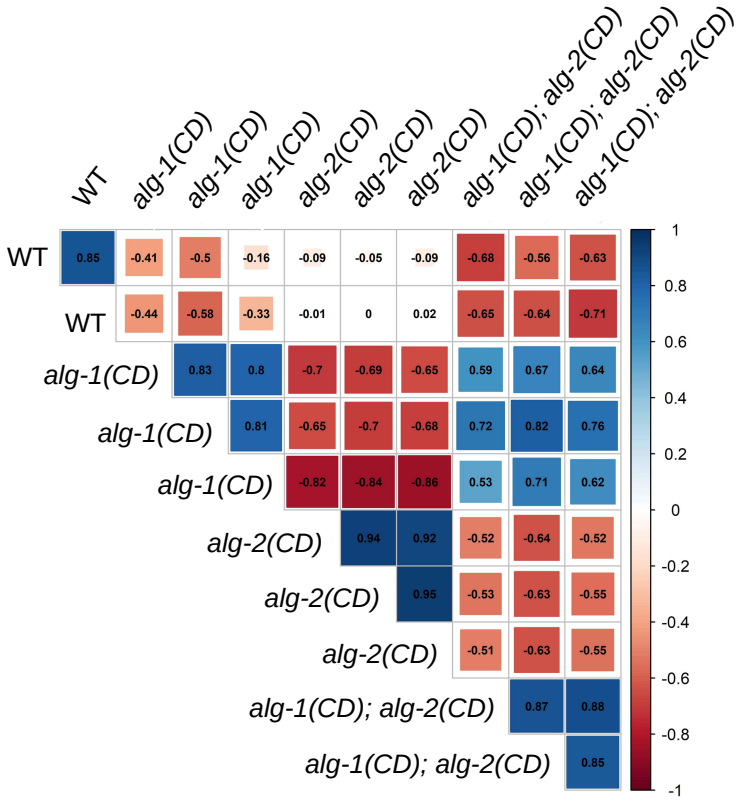
WT
alg-1(CD)
alg-1(CD)
alg-1(CD)
alg-2(CD)
alg-2(CD)
alg-2(CD)
alg-1(CD); alg-2(CD)
alg-1(CD); alg-2(CD)
alg-1(CD); alg-2(CD)
WT 0.85 -0.41 -0.5 -0.16 -0.09 -0.05 -0.09 -0.68 -0.56 -0.63
WT -0.44 -0.58 -0.33 -0.01 0 0.02 -0.65 -0.64 -0.71
alg-1(CD) 0.83 0.8 -0.7 -0.69 -0.65 0.59 0.67 0.64
alg-1(CD) 0.81 -0.65 -0.7 -0.68 0.72 0.82 0.76
alg-1(CD) -0.82 -0.84 -0.86 0.53 0.71 0.62
alg-2(CD) 0.94 0.92 -0.52 -0.64 -0.52
alg-2(CD) 0.95 -0.53 -0.63 -0.55
alg-2(CD) -0.51 -0.63 -0.55
alg-1(CD); alg-2(CD) 0.87 0.88
alg-1(CD); alg-2(CD) 0.85
1
0.8
0.6
0.4
0.2
0
-0.2
-0.4
-0.6
-0.8
-1

Figure S3

A

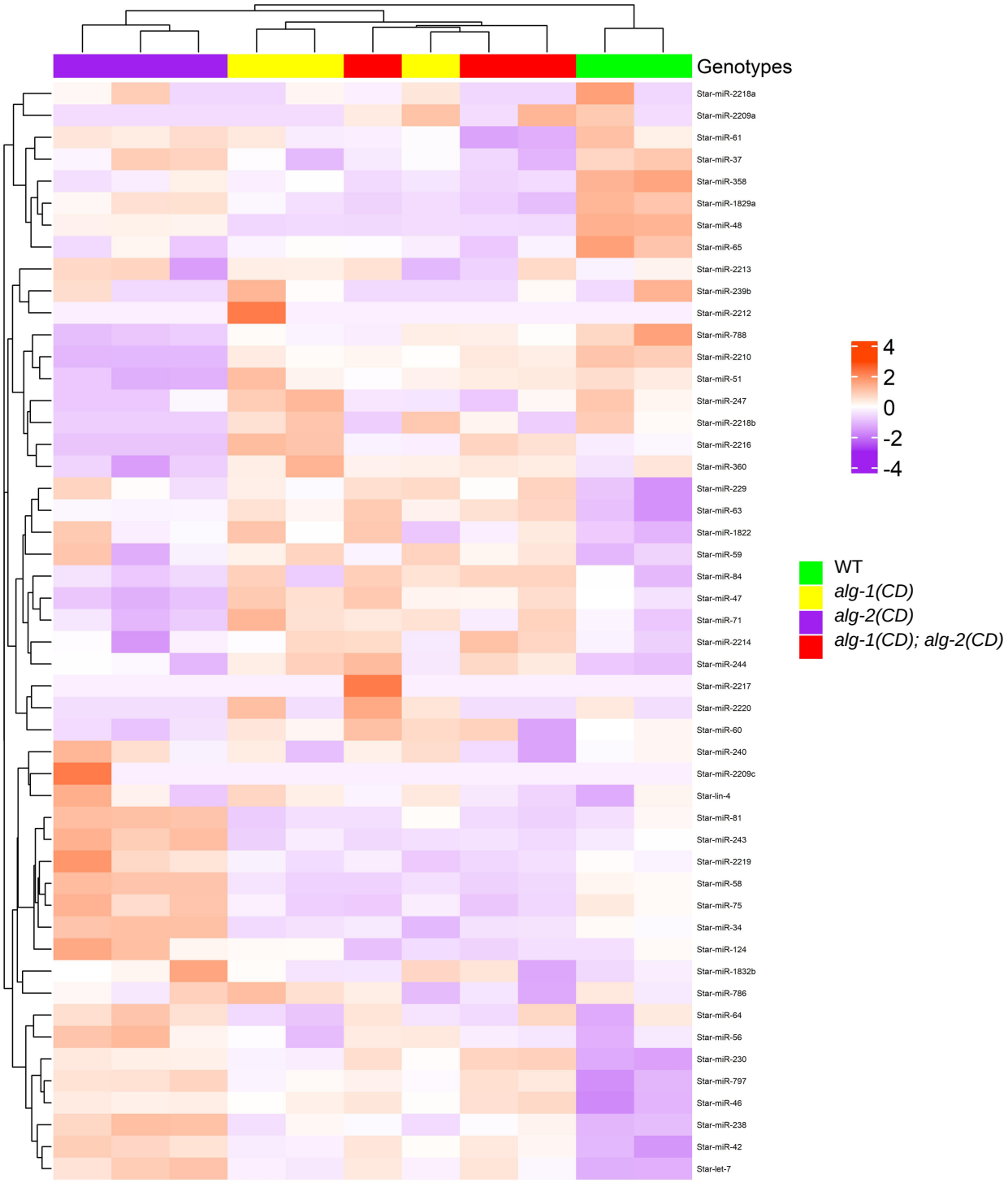
Genotypes
Star-miR-2218a
Star-miR-2209a
Star-miR-61
Star-miR-37
Star-miR-358
Star-miR-1829a
Star-miR-48
Star-miR-65
Star-miR-2213
Star-miR-239b
Star-miR-2212
Star-miR-788
Star-miR-2210
Star-miR-51
Star-miR-247
Star-miR-2218b
Star-miR-2216
Star-miR-360
Star-miR-229
Star-miR-63
Star-miR-1822
Star-miR-59
Star-miR-84
Star-miR-47
Star-miR-71
Star-miR-2214
Star-miR-244
Star-miR-2217
Star-miR-2220
Star-miR-60
Star-miR-240
Star-miR-2209c
Star-lin-4
Star-miR-81
Star-miR-243
Star-miR-2219
Star-miR-58
Star-miR-75
Star-miR-34
Star-miR-124
Star-miR-1832b
Star-miR-786
Star-miR-64
Star-miR-56
Star-miR-230
Star-miR-797
Star-miR-46
Star-miR-238
Star-miR-42
Star-let-7
4
2
0
-2
-4
WT
alg-1(CD)
alg-2(CD)
alg-1(CD); alg-2(CD)

Figure S4

B

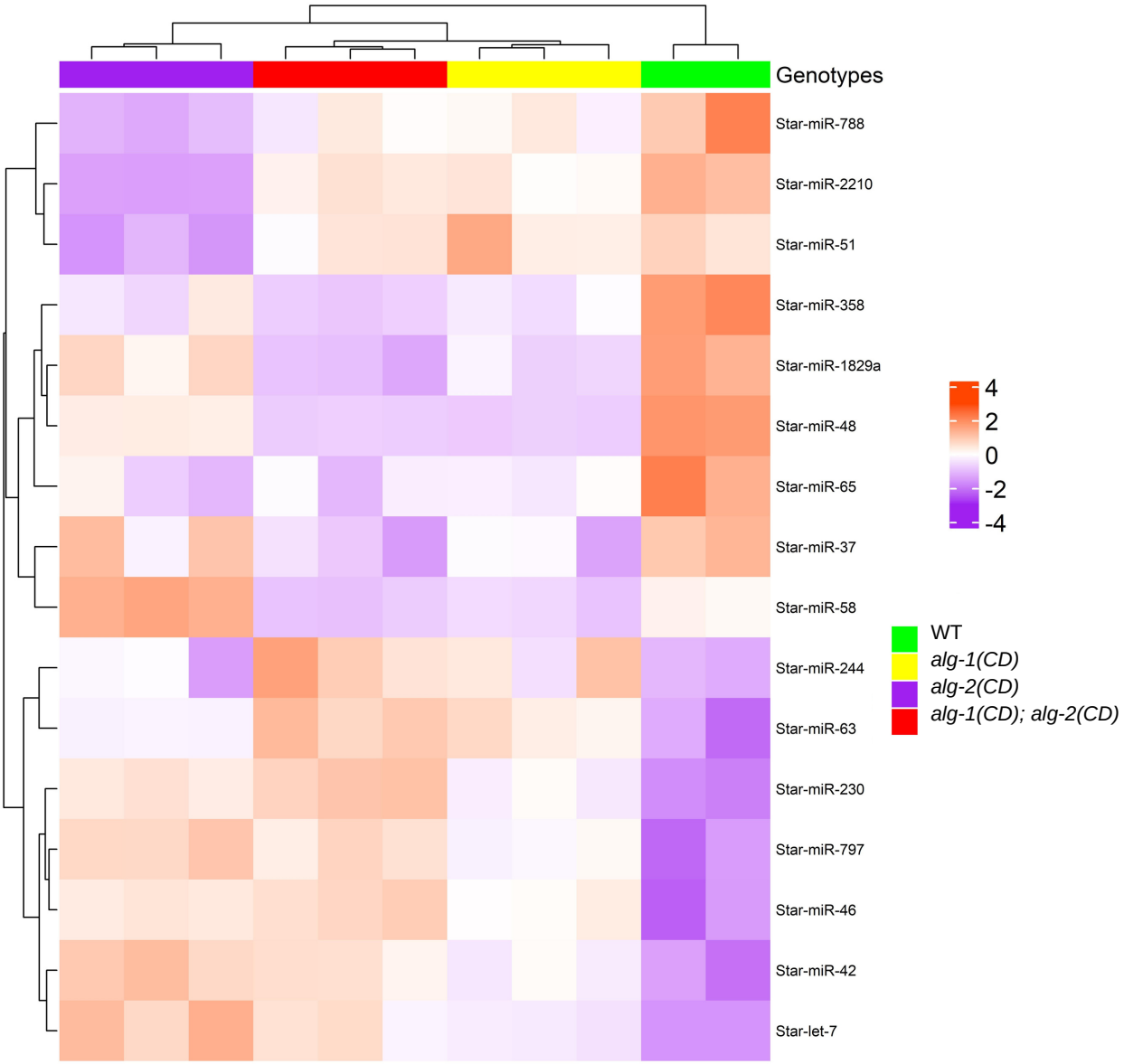
Genotypes
Star-miR-788
Star-miR-2210
Star-miR-51
Star-miR-358
Star-miR-1829a
Star-miR-48
Star-miR-65
Star-miR-37
Star-miR-58
Star-miR-244
Star-miR-63
Star-miR-230
Star-miR-797
Star-miR-46
Star-miR-42
Star-let-7
4
2
0
-2
-4
WT
alg-1(CD)
alg-2(CD)
alg-1(CD); alg-2(CD)

Figure S4

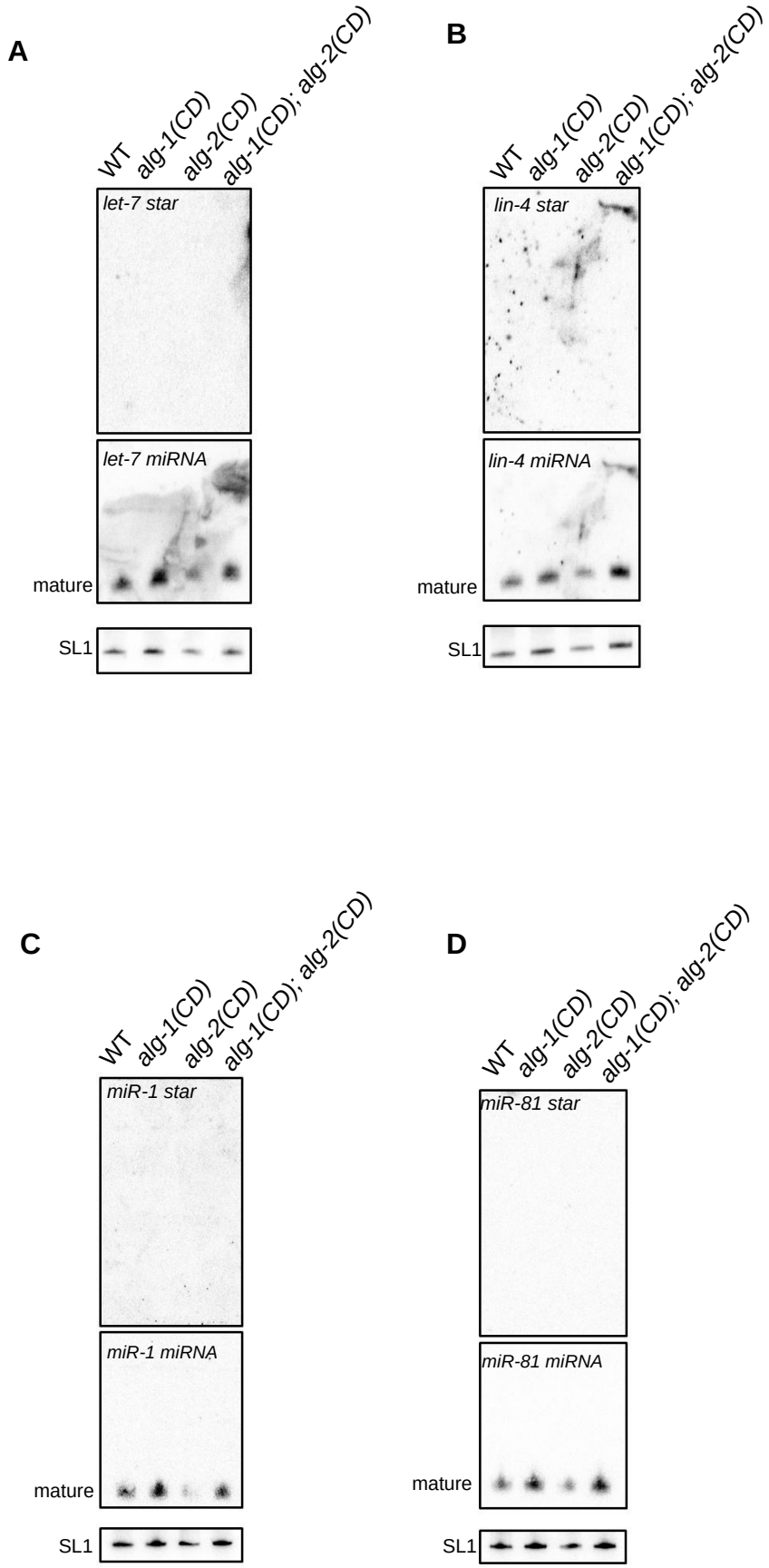
A
WT
alg-1(CD)
alg-2(CD)
alg-1(CD); alg-2(CD)
let-7 star
let-7 miRNA
mature
SL1
B
WT
alg-1(CD)
alg-2(CD)
alg-1(CD); alg-2(CD)
lin-4 star
lin-4 miRNA
mature
SL1
C
WT
alg-1(CD)
alg-2(CD)
alg-1(CD); alg-2(CD)
miR-1 star
miR-1 miRNA
mature
SL1
D
WT
alg-1(CD)
alg-2(CD)
alg-1(CD); alg-2(CD)
miR-81 star
miR-81 miRNA
mature
SL1

Figure S5

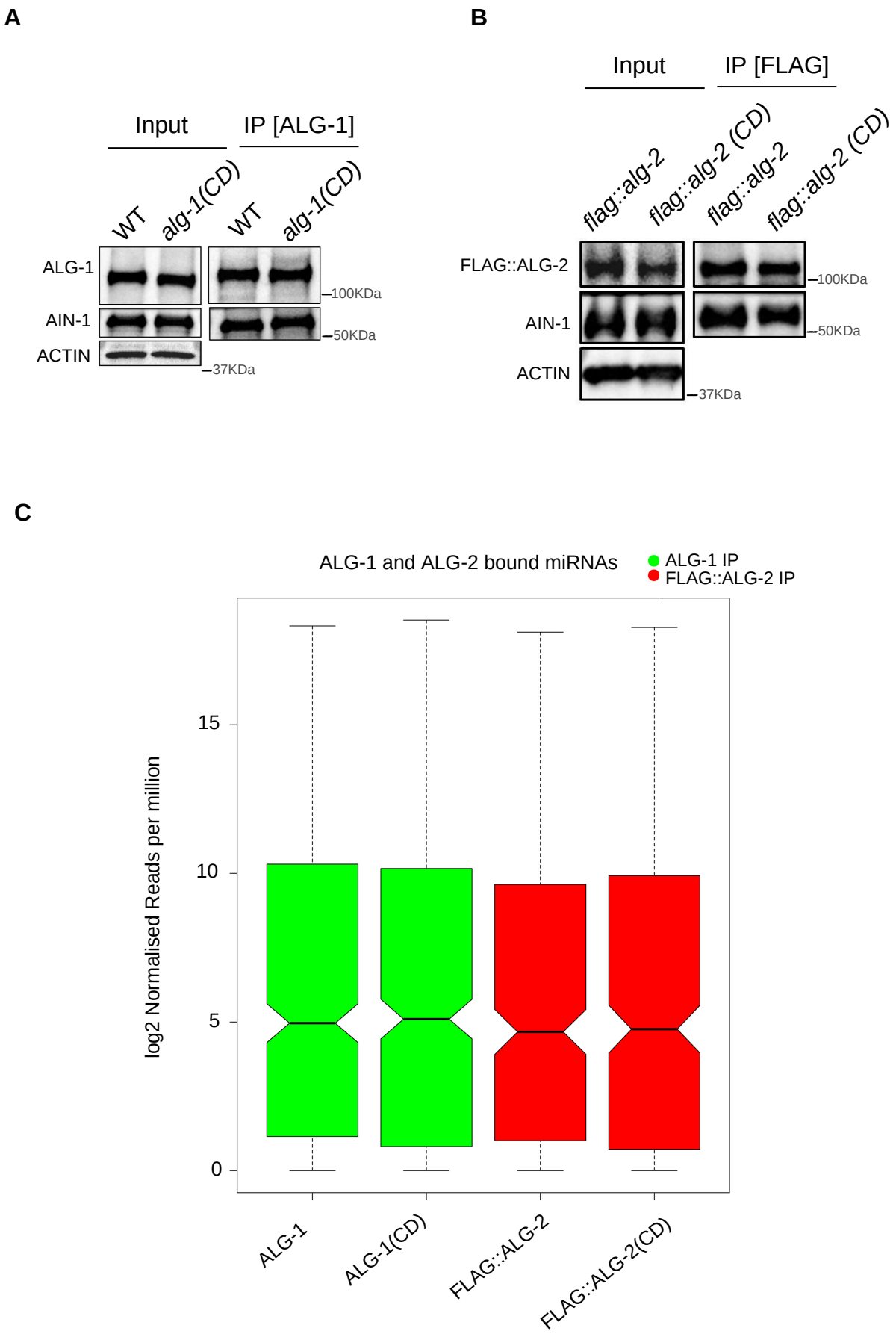
A
Input
IP [ALG-1]
WT
alg-1(CD)
WT
alg-1(CD)
ALG-1
AIN-1
ACTIN
100KDa
50KDa
37KDa
B
Input
IP [FLAG]
flag::alg-2
flag::alg-2 (CD)
flag::alg-2
flag::alg-2 (CD)
FLAG::ALG-2
AIN-1
ACTIN
100KDa
50KDa
37KDa
C
ALG-1 and ALG-2 bound miRNAs
ALG-1 IP
FLAG::ALG-2 IP
log2 Normalised Reads per million
0
5
10
15
ALG-1
ALG-1(CD)
FLAG::ALG-2
FLAG::ALG-2(CD)

Figure S6

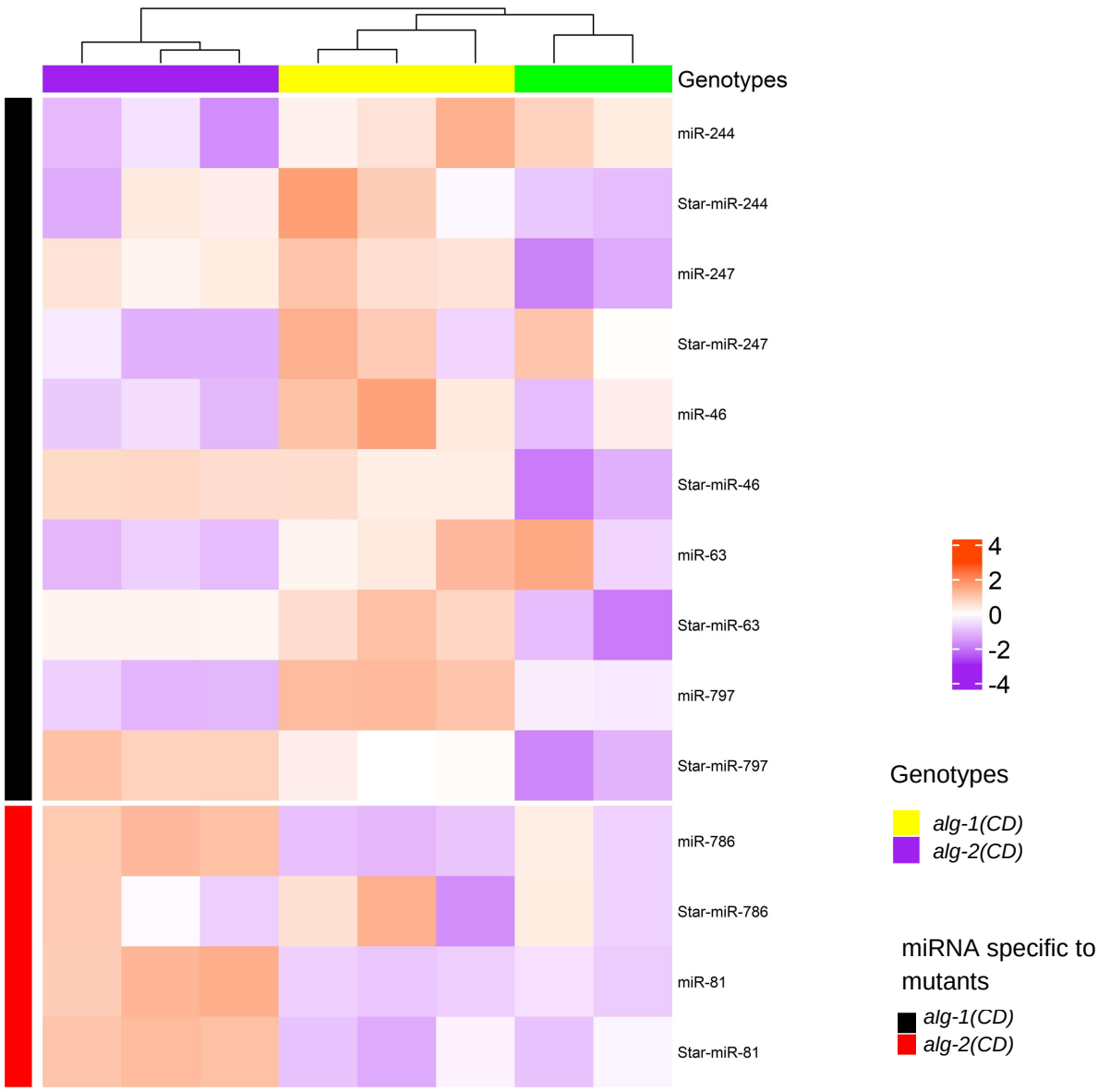
Genotypes
miR-244
Star-miR-244
miR-247
Star-miR-247
miR-46
Star-miR-46
miR-63
Star-miR-63
miR-797
Star-miR-797
miR-786
Star-miR-786
miR-81
Star-miR-81
4
2
0
-2
-4
Genotypes
alg-1(CD)
alg-2(CD)
miRNA specific to mutants
alg-1(CD)
alg-2(CD)

Figure S7